

RESEARCH

Open Access



Comparative efficacy of bio-selenium nanoparticles and sodium selenite on morpho-physiochemical attributes under normal and salt stress conditions, besides selenium detoxification pathways in *Brassica napus* L.

Ali Mahmoud El-Badri^{1,2}, Ahmed M. Hashem^{1,3}, Maria Batool¹, Ahmed Sherif^{1,2}, Elsayed Nishawy⁴, Mohammed Ayaad⁵, Hamada M. Hassan², Ibrahim M. Elrewainy², Jing Wang¹, Jie Kuai¹, Bo Wang^{1*}, Shixue Zheng⁶ and Guangsheng Zhou¹

Abstract

Selenium nanoparticles (SeNPs) have attracted considerable attention globally due to their significant potential for alleviating abiotic stresses in plants. Accordingly, further research has been conducted to develop nanoparticles using chemical ways. However, our knowledge about the potential benefit or phytotoxicity of bioSeNPs in rapeseed is still unclear. Herein, we investigated the effect of bioSeNPs on growth and physiochemical attributes, and selenium detoxification pathways compared to sodium selenite (Se (IV)) during the early seedling stage under normal and salt stress conditions. Our findings showed that the range between optimal and toxic levels of bioSeNPs was wider than Se (IV), which increased the plant's ability to reduce salinity-induced oxidative stress. BioSeNPs improved the phenotypic characteristics of rapeseed seedlings without the sign of toxicity, markedly elevated germination, growth, photosynthetic efficiency and osmolyte accumulation versus Se (IV) under normal and salt stress conditions. In addition to modulation of Na⁺ and K⁺ uptake, bioSeNPs minimized the ROS level and MDA content by activating the antioxidant enzymes engaged in ROS detoxification by regulating these enzyme-related genes expression patterns. Importantly, the main effect of bioSeNPs and Se (IV) on plant growth appeared to be correlated with the change in the expression levels of Se-related genes. Our qRT-PCR results revealed that the genes involved in Se detoxification in root tissue were upregulated upon Se (IV) treated seedlings compared to NPs, indicating that bioSeNPs have a slightly toxic effect under higher concentrations. Furthermore, bioSeNPs might improve lateral root production by increasing the expression level of *LBD16*. Taken together, transamination and selenation were more functional methods of Se detoxification and proposed different degradation pathways that synthesized malformed or deformed selenoproteins,

*Correspondence: wangbo@mail.hzau.edu.cn

¹ MOA Key Laboratory of Crop Ecophysiology and Farming System in the Middle Reaches of the Yangtze River, College of Plant Science & Technology, Huazhong Agricultural University, Wuhan 430070, People's Republic of China

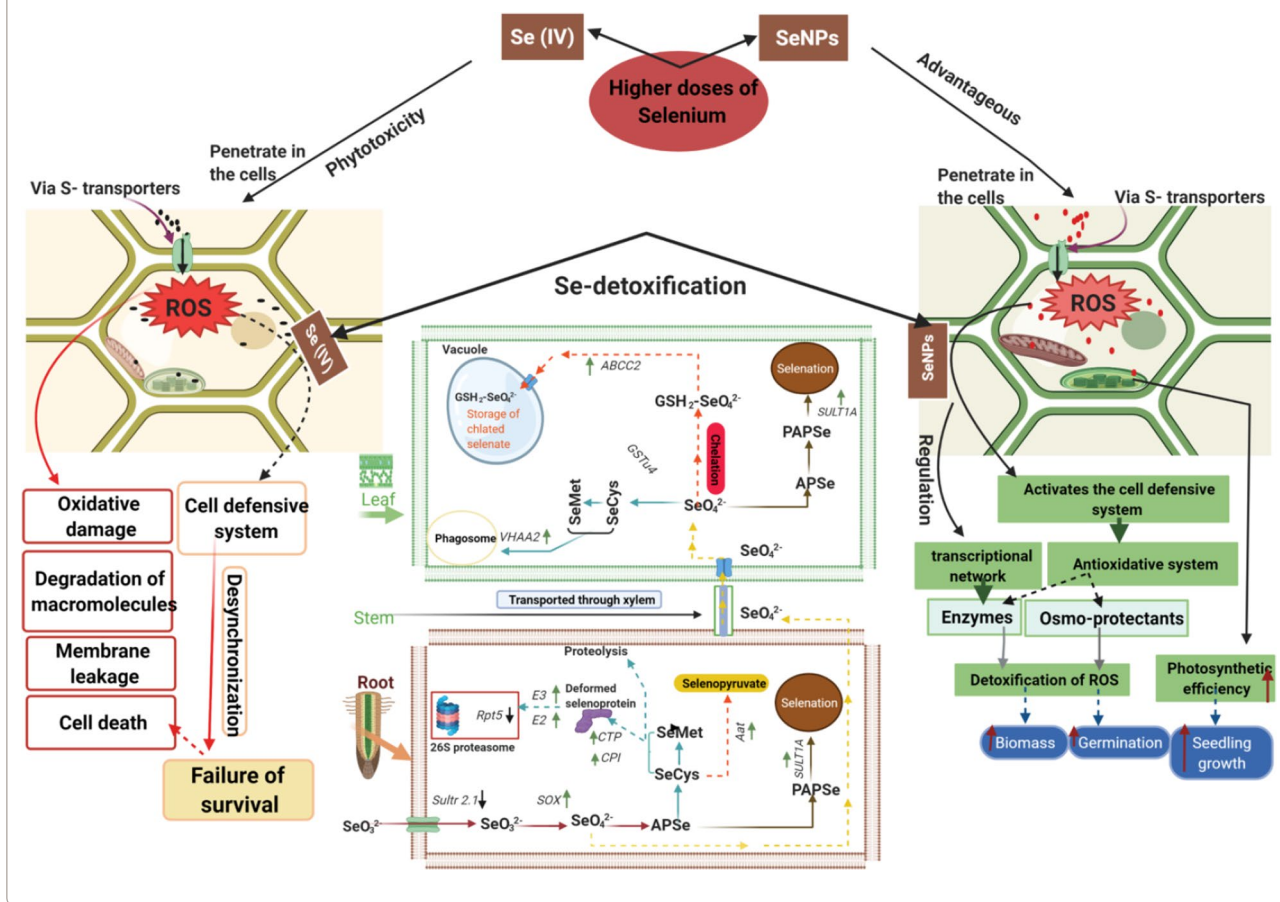
Full list of author information is available at the end of the article



which provided essential mechanisms to increase Se tolerance at higher concentrations in rapeseed seedlings. Current findings could add more knowledge regarding the mechanisms underlying bioSeNPs induced plant growth.

Keywords: Bio-selenium nanoparticles, Sodium selenite, Selenium detoxification, Salt stress, *Brassica napus* L.

Graphical Abstract



Introduction

Selenium is a fundamental and beneficial element for different organisms at low exposure levels and toxic at high concentrations with a narrow range between deficiency and excess [1]. Under lower doses, Se enhances the plant growth parameters by alleviating abiotic stresses effects such as organic and inorganic pollutants, salt stress, elevated temperature and water deficiency [2]. Selenium can enter directly or indirectly into the food chain mainly via plants; therefore, studying the impacts and fate of Se is significant for living organisms. Also, Se participates in the vital biological processes by synthesizing into selenoenzymes, which can improve the plant antioxidant activity, scavenge free radicals and protect the cell membrane [3]. On the contrary, Se with higher doses acts as a pro-oxidant, reducing yields and inducing metabolic disturbances [4]. The effects of Se in different tissues are

dependent on the exposure doses and type of Se [5]. Furthermore, Se uses the same pathway as sulfur (S) in the plant, and it's transported into plant tissues using S transporters and assimilated to selenocysteine (SeCys) or selenomethionine (SeMet); besides, Se might be methylated and converted into a non-toxic form [2, 6, 7] (Additional file 1: Fig. S1).

In the last decade, the application of several metal-based NPs such as ZnONPs [8], FeNPs and ZnNPs [9], TiO₂NPs [10], CuNPs [11] and AgNPs [12] reduced the harmful effects of respective metal elements in agriculture. It also reduced the cost of fertilizers and pesticides, improved the efficiency of chemical materials, enhanced the absorbance, transportation and transformation of these minerals from the soil into the plant; hence it improved the productivity of plants and bio-controlling [13, 14]. Nanotechnology has the potential

to revolutionize agriculture and play an important role in food and crop production [12, 15]. Compared to bulk materials, nanoparticles possess better physicochemical properties at optimum concentrations [16, 17].

Nanotechnology can assist the synthesis of different antioxidative compounds based upon their redox abilities using minerals, among them is Se, which was considered to rely on its red-ox abilities, owing to its various oxidation forms (+6, +4, +2, 0, -1, -2), besides that it also has a complicated antioxidative efficiency [18]. Selenium nanoparticles (SeNPs) were synthesized using biotic or abiotic pathways and widely occurred in the ambient, particularly in the heavy metallic mining regions [18]. The form of SeNPs is reported as novel compounds with lower toxicity compared with other seleno-species; additionally, it has better antioxidant properties due to the zero-oxidation state [19]. The significant effects of SeNPs on various species alter according to their different growth stages and exposure periods depending on SeNPs physicochemical composition [20]. SeNPs treatment reinforced plant growth in mustard, tomato and tobacco [13–15], improved POD activity, and reduced MDA content through ROS suppression and inhibiting free radical activity [21]. SeNPs play a promising role in various essential metabolic and physicochemical processes, thereby improving plant development [22]. Under the SeNPs application, no impact was found on the photosynthetic efficiency, demonstrated by its limited permeation in the leaf cells [23]. The stimulatory effects of SeNPs were due to their slow uptake but rapid oxidation to selenite (become organic forms SeCys and SeMet) inside the plant [24].

Salinity is one of the major abiotic environmental stresses affecting plant crops, which involved 7% of rain-fed and 30% worldwide irrigated agriculture, finally leading to a 65% loss of crop production [25]. Salinity affects plant growth due to the toxicity of Na^+ and decreases the uptake of essential nutrients, including calcium (Ca^{2+}) and potassium (K^+), which disrupt cellular structures and restrict growth [26]. A higher salt level causes both osmotic and ionic stresses, damaging the photosynthetic apparatus and physiological processes such as closing the stomata and reducing the leaf expansion [27]. Additionally, salinity-induced osmotic stress is often accompanied by secondary stresses, such as oxidative stress that is harmful to plant cells due to excessive ROS, osmotic imbalance and water deficiency, which result in ion toxicity in stressed plants [28].

The current findings visualized the beneficial role of SeNPs by improving photosynthesis and antioxidative responses with optimal supplementation during the early growth stages [29]. We need more research to systematically comprehend the different pathways and interactions

between selenium and plants, where studies on toxic effects and their conduct are still finite. Se's hyperaccumulation ability in *Brassicaceae*, *Asteraceae* and *Fabaceae* has been reported [2]. Several studies have investigated *Brassicaceae*, especially *B. napus*, as it is the secondary accumulator model of Se with no signs of toxicity up to 100–1000 mg Se Kg^{-1} DW [2]. *Brassica napus* L. is one of the world's most important sources of high-quality vegetable oils with vegetable protein diets for livestock and human nutrition [30].

In this study, we scrutinize the Se-prompted dual impact on the physicochemical and molecular mechanisms of rapeseed. Hence, we applied two forms of Se [Na_2SeO_3 (Se (IV)) and bioSeNPs] in the culture solution to estimate the phytotoxicity of higher selenium on seed germination and early seedling growth through morpho-physicochemical properties under normal and salt stress conditions. Besides, we investigated the selenium detoxification pathways in rapeseed seedlings under higher doses of selenium during the early seedling stage in *B. napus*.

Materials and methods

Preparation, purification and characterization of bio selenium nanoparticles (bioSeNPs)

A 1% culture of *Comamonas testosteroni* S44 was inoculated in the LB media (LB, Sigma) and incubated at 37 °C for 12 h, 10 mM sodium selenite [$(\text{Na}_2\text{Se}_2\text{O}_3)$ (Se (IV))] was added to the culture media and incubated at 28 °C for further 72 h. The appearance of red color indicating the production of elemental selenium. Precipitated cells were washed 2–3 times with ddH₂O (18.2 M Ω -cm) and lysed by ultrasonication followed by centrifugation at 12,000 rpm for 5 min at room temperature. The pellets were resuspended and centrifuged with 80% (w/v) sucrose to remove the biomass (Additional file 1: Fig. S2). After that, the pellets were washed twice with ddH₂O to purify the bioSeNPs and kept at - 20 °C [31, 32].

To understand the characterization of bioSeNPs, the size distribution (DLS) and zeta potential were determined using zetasizer 2000 (UK). BioSeNPs were prepared for fourier transform infrared (FTIR) spectroscopy analysis. The sample was mixed with spectroscopic grade potassium bromide (KBr, dried for 24 h at 60 °C) in a ratio of 1:100, and the spectrum was recorded in the range of 400–4000 wavenumber (cm^{-1}) on the FTIR spectrometer, Spectrum 100 (Perkin Elmer, USA) in the diffuse reflectance mode at a resolution of 4 cm^{-1} in KBr pellets.

Structural properties of bioSeNPs were measured by scanning electron microscopy (SEM) using a Philips JSM 6390 model (USA) electron microscope and transmission

electron microscopy (TEM) (JEM-2100F, JEOL Inc.) at an accelerating voltage of 15 kV and 200 kV, respectively.

Plant material and treatment conditions

The mature seeds of rapeseed cultivar Yangyou 9 [Chinese rapeseed cultivar (扬油9号) collected from Jiangsu Lixiahe Agricultural Research Institute] were sterilized with 5% NaClO for five minutes then washed by ddH₂O 4–5 times. Seeds of uniform size were selected to minimize errors in seed germination and seedling vigor. To investigate the effect of bioSeNPs and Se (IV) on *B. napus* under standard and salt stress conditions, 60 sterilized seeds were placed on filter paper in the germination boxes (15 × 10 × 5 cm), containing 15 mL of different solutions, ddH₂O as a control and 50, 100 and 150 μmol L⁻¹ Se (IV) or bioSeNPs (standard conditions), ddH₂O, 150 and 200 mM NaCl as a control, 50, 100 and 150 μmol L⁻¹ Se (IV) or bioSeNPs combined with 150 and 200 mM NaCl (salt stress conditions). Three replicates of seeds were kept according to a randomized block design in a growth chamber with optimal conditions (day/night temperature at 25 ± 1/20 ± 1 °C) with 12 h light (13,000 lx) and 12 h dark (HP250GS-C, Ruihua Instrument and Equipment Co., Ltd., Wuhan, China) according to [33]. Germinated seeds were counted daily, starting from the first day of cultivation to the seventh day; seeds were considered germinated when the primary root was at least 2 mm long. All samples were collected and stored at -80 °C to determine physiochemical attributes.

Morphological characters

The final germination percentage (FG%), germination rate (GR), vigor index I (VI (I)) and vigor index II (VI (II)) were measured according to the equations reported by [12, 34].

After seven days of treatments, plants were harvested and separated into shoots and roots to measure lengths and fresh weight then dried to a constant weight at 80 °C for dry weight measurements [35].

Measurement of photosynthetic pigments

The contents of total chlorophyll and carotenoids in fresh samples were determined according to the formulae suggested by [36, 37].

Total soluble protein, total soluble sugar, malondialdehyde (MDA) and proline contents

Total soluble protein content was measured following [38] with BSA as a standard protein. At the same time,

the total soluble sugar content was estimated according to [39]. MDA content was measured using thiobarbituric acid (TBA), as mentioned by [40]. The absorbance of proline content was measured at 520 nm using toluene as a blank, according to [41].

Determination of H₂O₂ and O₂⁻ by NBT and DAB staining

3,3'-Diaminobenzidine (DAB, 1 mg mL⁻¹) and Nitro-tetrazolium blue (NBT, 1 mg mL⁻¹) staining were used to detect H₂O₂ and O₂⁻ levels, respectively, in leaves and roots. DAB and NBT staining were performed as described by [42, 43].

RNA extraction, cDNA synthesis and quantitative RT-PCR

Seven-day after germination of *B. napus*, shoots and roots were collected and immediately frozen in liquid nitrogen for RNA extraction. Total RNA extraction was performed using TransZol Up reagent (TransGen, Beijing, China). Concentration and quality of RNA were determined with a Nanodrop 2000 Spectrophotometer (Thermo Fisher Scientific). cDNA was synthesized from 1 μg of RNA using TransScript One-Step gDNA Removal and cDNA Synthesis SuperMix kit (TransGen, Beijing, China) following the manufacturer's instructions. cDNA was diluted 1:10 for quantitative real-time PCR (qRT-PCR).

Quantitative real-time PCR analyses were performed using TransStart Tip Green qPCR SuperMix (TransGen, Beijing, China) with Roche LightCycler 480 thermal cycler instrument, 384-well (Roche). Relative expression values were calculated using the 2^{-ΔΔCt} method according to [44, 45], β-ACTIN was used as a reference gene, primers are listed in Additional file 1: Table S1. Three biological replicates were performed for each sample, and three technical replicates represented each biological replicate.

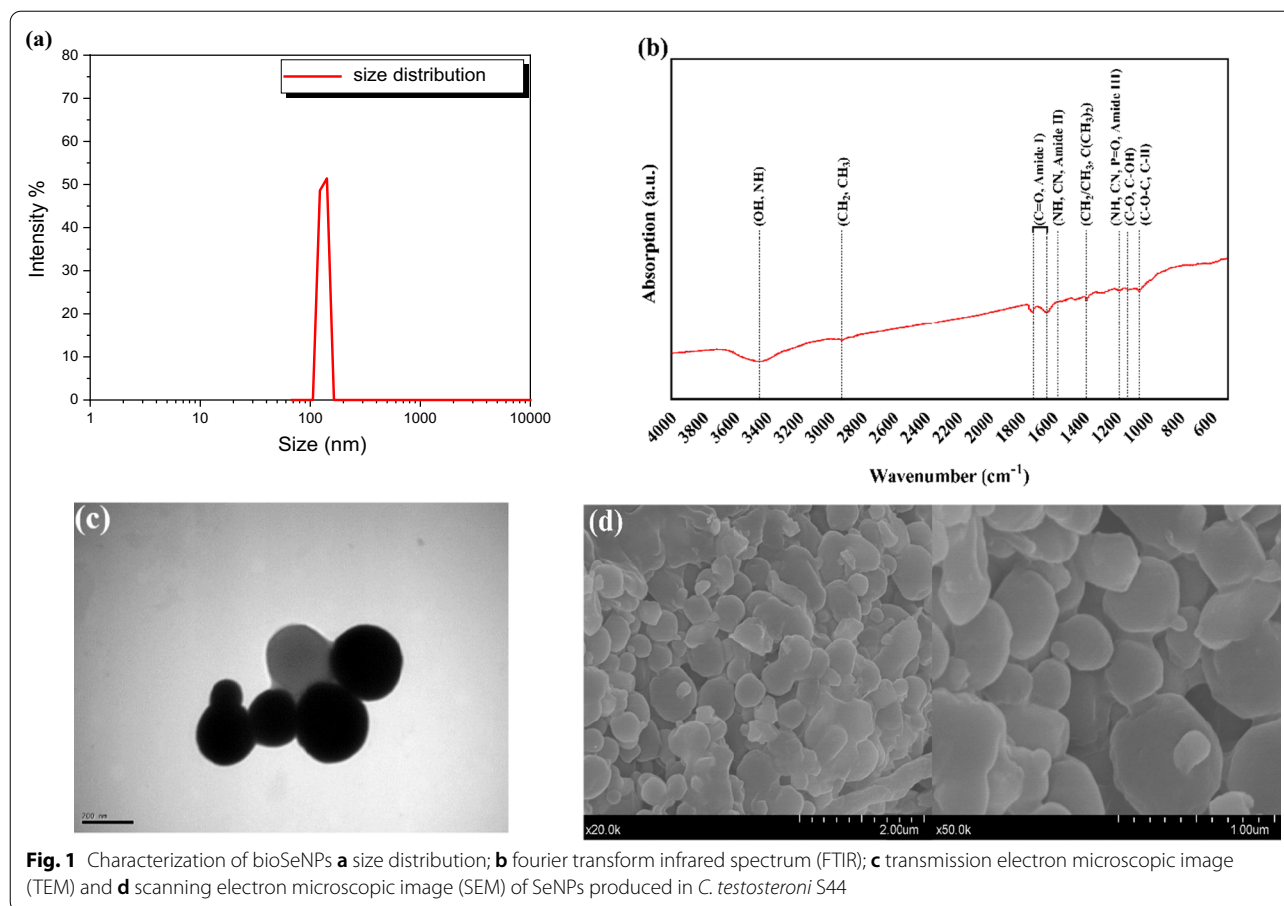
Statistical analysis

The data for each variable were subjected to analysis of variance. The significance of differences between the control and the treatment mean values were determined by the Duncan's Multiple Range Test (DMRT) at *P* < 0.05 significance level. The graphical presentation was carried out using GraphPad prism (V8.0.1) and RStudio software. The values presented are the means of three independent experiments.

Results

BioSeNPs characterization

Dynamic Light Scattering (DLS) analysis showed that the size of bioSeNPs was ranged from 120 to 260 nm with an average size of 167 nm (Fig. 1a). However, a few bioSeNPs



displayed an extremely big size. The possible explanation could be that a high concentration of bioSeNPs formed large aggregates; meanwhile, zeta potential analysis indicates that bioSeNPs displayed a negative potential of -32.4 ± 2 mV in ddH₂O.

Fourier transform infrared (FTIR) spectroscopic analysis of bioSeNPs ranged from 400 to 4000 cm^{-1} (Fig. 1b). The FTIR spectrum of NPs exhibited peaks at 3446 cm^{-1} attributed to -OH and -NH stretching of protein, carbohydrates and lipids, and 2926 cm^{-1} can be ascribed to CH₂ and CH₃ stretching from lipids and proteins. Additionally, the strongest and sharp features at 1723 and 1638 cm^{-1} confirmed C=O stretching vibration present in proteins (amide I). The other band observed at 1567 cm^{-1} corresponded to N-H and C-N stretching vibrations, illustrating the presence of peptide bonds in different protein conformations (amide II). A sharp peak at 1385 cm^{-1} indicated the presence of CH₂/CH₃ and C(CH₃)₂ stretching mainly in proteins and lipids. The C-N stretching and N-H bending vibrations were also observed at 1181 cm^{-1} (amide III), which reflected the presence of the $\nu_{\text{asym}} \text{PO}_2^-$ in nucleic acid and phospholipids on bioSeNPs. On the

other side, small features of bioSeNPs at 1055 cm^{-1} (C-O-C and C-H) and 1128 cm^{-1} (C-O, C-OH) characterized to carbohydrates (Fig. 1b), these assignments are based on earlier research [31, 46, 47]. Conclusively, FTIR spectra confirmed the presence of various capping biomacromolecules (proteins, carbohydrates and lipids) at the SeNPs surface.

The morphology of biosynthesized SeNPs was visualized by transmission electronic microscopy (TEM) and scanning electronic microscopy (SEM) are shown in (Fig. 1c, d); bioSeNPs have a spherical architecture with an average diameter size ranging from 120 to 260 nm (TEM), and from 175 to 400 nm (SEM). Moreover, it was reported that the size of bioSeNPs was ranged from 120 to 300 nm [48].

BioSeNPs enhanced seed germination and seedling growth

We exogenously applied different concentrations of bioSeNPs and Se (IV) (0, 50, 100 and 150 $\mu\text{mol L}^{-1}$) to investigate the effect of Se (higher doses) on seed germination and seedling growth of *B. napus*. Our results demonstrated that the nano-solutions treatment accelerated

the seed germination compared to sodium selenite and control. The final germination percentage (FG%) was significantly increased by 1.06, 1.30 and 1.27% under 50, 100 and 150 $\mu\text{mol L}^{-1}$ doses of bioSeNPs versus control, respectively, while decreased by 0.86, 2.46 and 2.90% under 50, 100 and 150 $\mu\text{mol L}^{-1}$ doses of Se (IV), respectively, compared to control (Fig. 2a). Interestingly, treated seeds with bioSeNPs, especially 150 $\mu\text{mol L}^{-1}$, recorded the highest value of 94.88, 984.1 and 44.18% for germination rate (GR), vigor index I (VI (I)) and vigor index II (VI (II)), respectively, when compared to those of Na_2SeO_3 and control (Fig. 2a).

Furthermore, we investigated the effect of bioSeNPs on the phenotype of *B. napus* seedlings. We observed that after 7-days of exposure to bioSeNPs, plant growth was stimulated with no sign of toxicity, while the sodium selenite (Se (IV)) treatment showed wilt and stunted shoot and root growth compared to control (Fig. 2b).

Our results showed that 150 $\mu\text{mol L}^{-1}$ bioSeNPs increased the shoot and root length by 8.47 and 24.74%, respectively, whereas Na_2SeO_3 (150 $\mu\text{mol L}^{-1}$) decreased shoot and root length by 7.85 and 67.47% versus control, respectively (Fig. 2c, d). As compared to control, shoot fresh weight was significantly increased by 1.59, 3.10 and 4.49% under 50, 100 and 150 $\mu\text{mol L}^{-1}$ of bioSeNPs, respectively, while it was decreased by 1.47, 4.32 and 6.89% under 50, 100 and 150 $\mu\text{mol L}^{-1}$ of Na_2SeO_3 , respectively (Fig. 2e). Besides, nano-treatments also increased the root fresh weight by 22.8% (50 $\mu\text{mol L}^{-1}$), 24.24% (100 $\mu\text{mol L}^{-1}$) and 25.5% (150 $\mu\text{mol L}^{-1}$) versus control with the non-significant difference among the NPs concentrations. On the other side, Na_2SeO_3 reduced the root fresh weight by 51.87, 78.45 and 87.62% under 50, 100 and 150 $\mu\text{mol L}^{-1}$, respectively, versus control (Fig. 2f). Additionally, Na_2SeO_3 treatments increased shoot dry weight by 29.56, 25.57 and 26.94%, while decreased root dry weight by 40.68, 63.52 and 71.42% under 50, 100 and 150 $\mu\text{mol L}^{-1}$ versus control, respectively. In contrast, bioSeNPs have a non-significant effect on the shoot and root dry weight compared to relative control (Additional file 1: Fig. S3a, b).

Twofold effects of two Se forms on photosynthetic pigments, osmoprotectants, MDA and proline contents

To investigate the effect of bioSeNPs and Na_2SeO_3 on photosynthesis, we analyzed the contents of the

photosynthetic pigments upon Se treatments (Fig. 3a–d). Chlorophyll content was affected by Se application in both forms, especially on the higher concentration of Se (150 $\mu\text{mol L}^{-1}$), which increased chlorophyll a, chlorophyll b and total chlorophyll contents by 21.83, 24.85 and 24.04% (bioSeNPs), while declining by 5.22, 11.14 and 8.19% (Na_2SeO_3), respectively, compared to the control (Fig. 3a–c). Moreover, carotenoids content dramatically increased with increasing the Se concentrations by 108.7, 151.3 and 164.6% (Na_2SeO_3), and by 23.13, 35.97 and 27.45% (bioSeNPs), under 50, 100 and 150 $\mu\text{mol L}^{-1}$ versus control, respectively (Fig. 3d).

Our investigation demonstrated that the total soluble sugars (TSS) content showed a decreased trend with increasing Se concentrations. BioSeNPs decreased the TSS content by 6.01, 5.85 and 2.11%, and a large reduction was observed when Na_2SeO_3 was applied by 7.48, 16.89 and 28.48% under 50, 100 and 150 $\mu\text{mol L}^{-1}$ versus control, respectively (Fig. 3e). Our results indicated a negative effect of Se on total soluble protein content (TSP) at the tested concentrations, which decreased by 8.48, 4.81 and 5.86% (bioSeNPs), 15.52, 27.81 and 38.05% (Na_2SeO_3) under 50, 100 and 150 $\mu\text{mol L}^{-1}$ versus control, respectively (Fig. 3f).

The data (Fig. 3g) showed an increase in proline content corresponding to Se concentrations. The proline content showed significant increased by 21.60, 29.23 and 33.14% (bioSeNPs), 86.40, 125.69 and 243.38% (Na_2SeO_3) under 50, 100 and 150 $\mu\text{mol L}^{-1}$, respectively, over the control. The same trend was observed for lipid peroxidation content; results showed significant differences in MDA among tested Se treatments. The high Se doses (150 $\mu\text{mol L}^{-1}$) increased MDA content by 23.07 and 57.94% for bioSeNPs and Na_2SeO_3 , respectively (Fig. 3h). Besides, bioSeNPs treatments showed lower MDA content than the Na_2SeO_3 treatments.

Assessment of ROS accumulation and antioxidant enzyme genes expression under Se treatment

After seven days of Se treatments, we investigated the accumulation of H_2O_2 and $\text{O}_2^{\cdot-}$ in leaves and roots in rapeseed using nitro blue tetrazolium (NBT) and 3,3-diaminobenzidine (DAB), respectively. Results for DAB staining showed that Se (IV) treatments resulted in a darker brown color staining in leaves and roots than nano-treated, which elucidates the greater production

(See figure on next page.)

Fig. 2 Effect of two selenium forms (SeNPs and Se (IV)) on rapeseed seedlings (Yangyou 9) during the early seedling stage. **a** impacts of selenium treatments on the germination characteristics (FG%: final germination percentage, GR: germination rate, VI (I): vigor index I and VI (II): vigor index II). SeNPs stimulated seedling growth. **b** Different concentrations of SeNPs and Se (IV) (0, 50, 100 and 150 $\mu\text{mol/L}$) differentially affected rapeseed seedlings phenotype. Scale bar = 1 cm. **c–f** Impact of selenium treatments on **c** shoot length (cm); **d** root length (cm); **e** shoot fresh weight (g) and **f** root fresh weight (g) under different concentration of SeNPs and Na_2SeO_3 (0, 50, 100 and 150 $\mu\text{mol/L}$) during the early seedling stage. Bars represent \pm SE of three replicates. The different letters indicate significant differences at $P < 0.05$ using Duncan's multiple range tests

(a)

Concentrations	Treatments	FG%	GR	VI (I)	VI (II)
0 $\mu\text{mol/L}$	Control	98 \pm 0.59 ^{bc}	93.02 \pm 0.32 ^b	808.4 \pm 2.90 ^c	38.33 \pm 0.86 ^c
	SeNPs	99 \pm 0.55 ^{ab}	93.59 \pm 0.67 ^{ab}	956.5 \pm 7.20 ^b	41.57 \pm 0.57 ^b
50 $\mu\text{mol/L}$	Se (IV)	97 \pm 0.82 ^{cd}	92.72 \pm 0.71 ^{bc}	496.6 \pm 2.61 ^d	36.48 \pm 0.52 ^d
	SeNPs	100 \pm 0.53 ^a	93.74 \pm 0.76 ^{ab}	972.9 \pm 1.15 ^{ab}	42.65 \pm 0.67 ^{ab}
100 $\mu\text{mol/L}$	Se (IV)	96 \pm 0.86 ^{de}	91.66 \pm 0.64 ^c	330.4 \pm 5.60 ^e	30.81 \pm 0.89 ^e
	SeNPs	100 \pm 0.75 ^a	94.88 \pm 0.69 ^a	984.1 \pm 4.72 ^a	44.18 \pm 0.49 ^a
150 $\mu\text{mol/L}$	Se (IV)	95 \pm 0.82 ^e	91.43 \pm 0.37 ^c	272.1 \pm 2.52 ^f	27.61 \pm 0.45 ^f

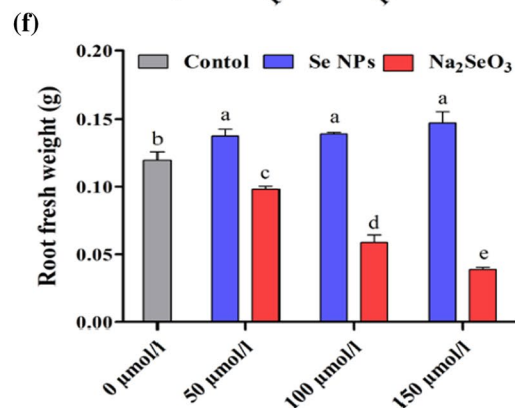
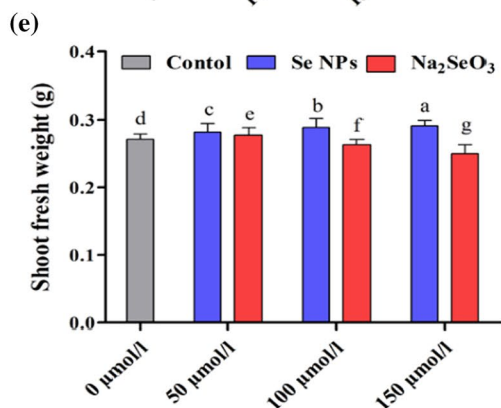
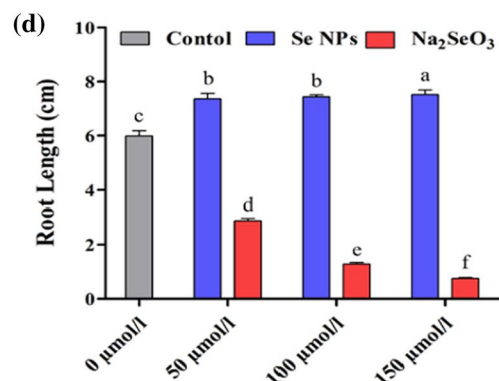
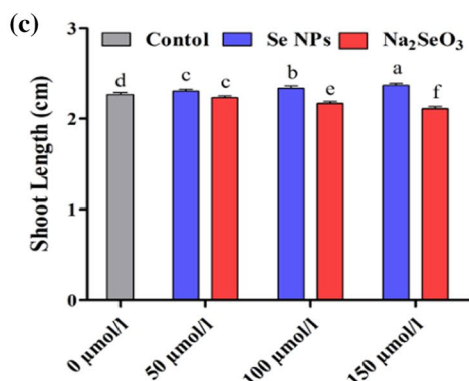
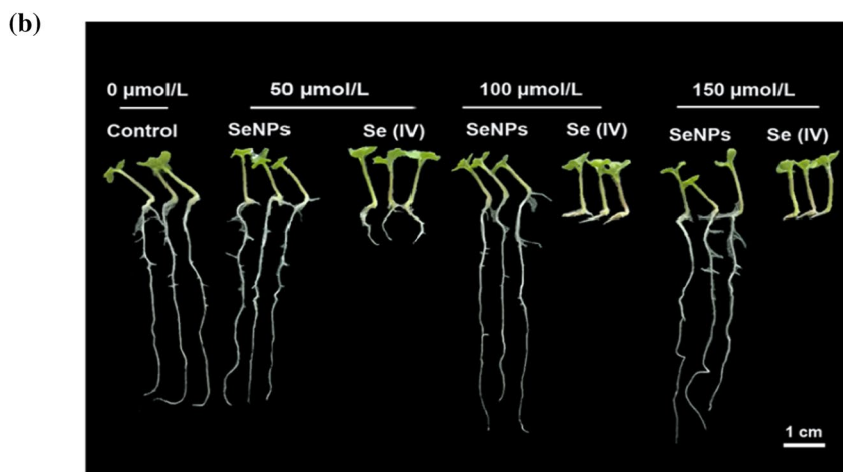
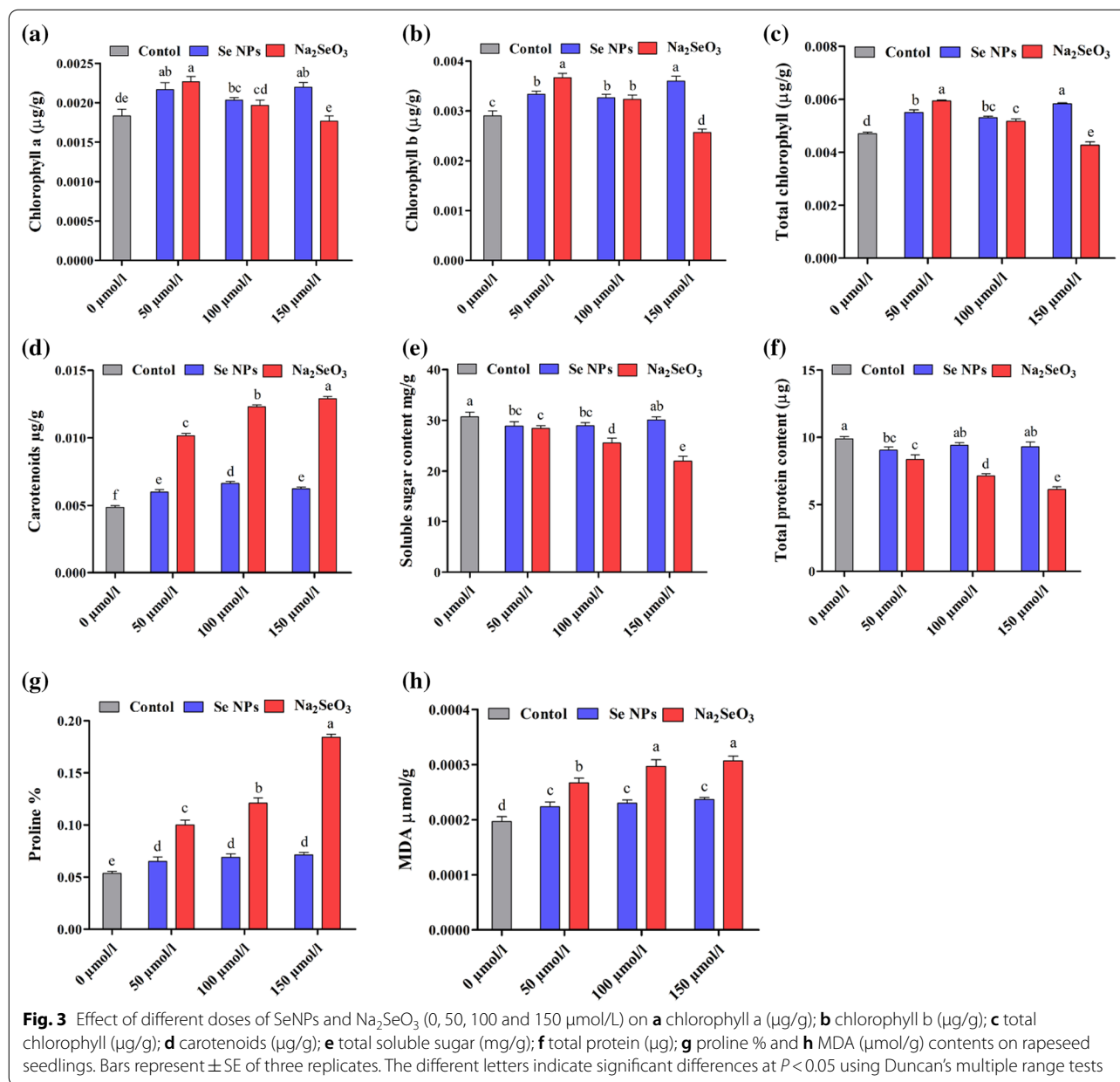


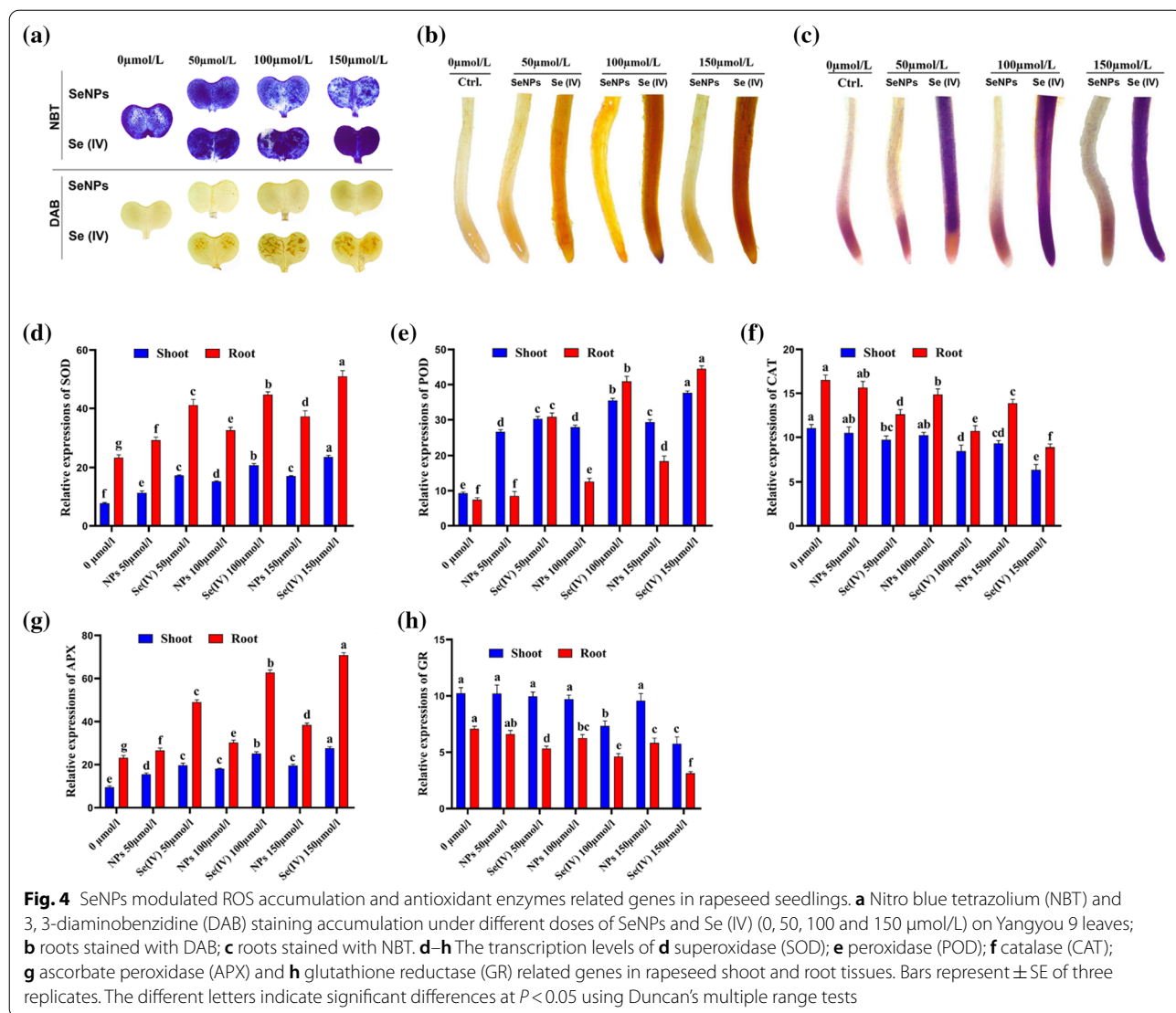
Fig. 2 (See legend on previous page.)



and accumulation of excessive H₂O₂ in Se (IV) as compared to bioSeNPs at the same concentrations. Furthermore, the dark blue color of NBT staining represented a higher accumulation of O₂^{•-} under Se (IV); meanwhile, the bioSeNPs treated seedling did not show an obvious effect on H₂O₂ and O₂^{•-} accumulation in leaves and roots compared to control (Fig. 4a–c).

In this study, the transcript abundance of genes encoding antioxidant enzymes was differentially changed. After seven days of treatments, *B. napus* shoot and root tissues were harvested and used to determine

the expression levels of *SOD*, *POD*, *APX*, *CAT* and *GR* genes under different doses of bioSeNPs or Se (IV). The relative mRNA levels of *SOD*, *POD* and *APX* were up-regulated by 204.0, 305.2 and 191.0% (shoots), 177.1, 500.1 and 205.2% (roots), and down-regulated by 42.22 and 43.83% (shoots), 46.30 and 55.66% (roots) with *CAT* and *GR* under 150 µmol L⁻¹ of Se (IV) versus control, respectively (Fig. 4d–h). On the other hand, under higher concentration (150 µmol L⁻¹) of bioSeNPs, the expression pattern of these enzyme related genes was an increment in *SOD*, *POD* and *APX* by 119.0, 216.0 and 106.1% (shoots), 59.39, 148.00 and 65.73% (roots),

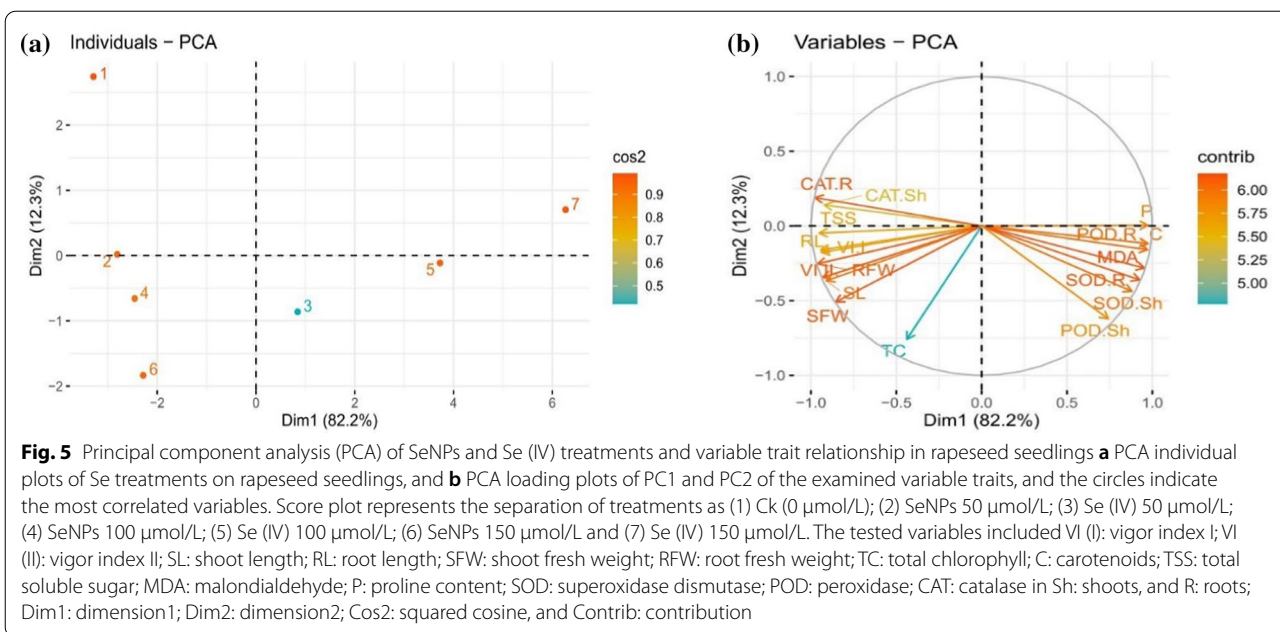


respectively, while transcript level of *CAT* and *GR* genes was decreased by 15.84 and 6.40% (shoots), and 16.03 and 17.62% (roots), respectively, versus control (Fig. 4d–h).

Impacts of Se application on growth during the early seedling stage

BioSeNPs boosted the germination parameters and growth traits under increased concentrations, with slight significance among the nano concentrations. In contrast, Se (IV) prominently inhibited the germination and growth traits and the maximum reduction in growth was expressly noted under the highest dose (150 $\mu\text{mol L}^{-1}$). Moreover, total chlorophyll contents were affected by Se application, especially on the higher doses (150 $\mu\text{mol L}^{-1}$) of bioSeNPs (increased) and Se (IV) (declined), while

carotenoids content dramatically elevated by increasing the Se concentration versus control (Additional file 1: Fig. S4a–c). Similarly, all osmotic adjustment parameters were significantly influenced by maximum inhibition at 150 $\mu\text{mol L}^{-1}$ compared to other treatments. The relative mRNA level of *SOD*, *POD*, and *APX* was up-regulated and down-regulated in *CAT* and *GR* under the highest Se (IV) doses in shoot and root tissues than relative control. The expression pattern of these enzyme-related genes was increased for *SOD*, *POD*, and *APX* in shoot and root tissues, while the transcript level of *CAT* and *GR* genes was decreased in shoots and roots under 150 $\mu\text{mol L}^{-1}$ of bioSeNPs (Additional file 1: Fig. S4a–c).



Principal component analysis of Se treated rapeseed plants

All the 17 traits were loaded into two major principal components (PC1 and PC2), explaining 94.5% of the total variances. Most of the examined traits were discriminated by PC1, which was explained by the larger proportions of variances (82.2%), while the lower proportions of variances (12.3%) were indicated by PC2 (Fig. 5a, b). Doses distribution visualized a clear signal of elevated levels of bioSeNPs, which recorded significant positive effects on the studied characteristics of rapeseed, contrary to that of Se (IV), which recorded negative effects during the early seedling stage. Specifically, bioSeNPs were more displaced from the other treatments, indicating alleviation of the elemental toxicity on the seeds and enhanced germination and early seedling growth. In contrast, 150 $\mu\text{mol L}^{-1}$ of Se (IV) was more displaced from the other treatments indicating increased elemental toxicity on the seeds and decreased germination and early seedling growth (Fig. 5a).

The loading plot classified the studied traits into three main groups depending on the two-dimensional plots. The CAT activity in shoot and root was positively correlated with Dim2, while MDA, proline and carotenoids

contents were positively associated with Dim1. The variable MDA (lipid peroxidation) has positive loadings for PC1 (82.2% of the total variance), which confirmed that MDA content was strongly correlated (negatively) to germination and growth-related traits, including vigor index (I), vigor index (II), shoot, root fresh and dry weight, shoot, root length and total chlorophyll. On the other hand, it is revealed that almost all the growth traits are positively correlated to each other with varying degrees of relationship, while all these variables are negatively correlated to the oxidative biomarkers, including SOD and POD in shoots and roots (Fig. 5b).

Impacts of Se treatments on the germination traits under two concentrations of NaCl

The findings of this study indicated that salt stress decreased the seeds germination by 2.08% (150 mM) and 6.21% (200 mM), which is more prominent under a higher stress level when comparing NaCl and CK. Whereas, supplementation of bioSeNPs increased the FG% by 3.18% (150 mM) and 3.68% (200 mM), while Se (IV) slightly decreased the FG% by 2.12% (150 mM) and 1.84% (200 mM) with 150 $\mu\text{mol L}^{-1}$ versus the seedling

(See figure on next page.)

Fig. 6 Nano-Se improves seedling growth under two different concentrations of NaCl. **a** Impact of selenium treatments on the germination characteristics [FG%: final germination percentage; GR: germination rate; VI (I): vigor index I and VI (II): vigor index II] under two concentrations of salt stress. **b** and **c** Seven-day-old seedlings phenotypes grown under two NaCl concentrations: **b** 150 mM NaCl and **c** 200 mM NaCl combined with different levels of SeNPs and Se (IV) (0, 50, 100 and 150 $\mu\text{mol/L}$). Scale bar = 1 cm. **d-g** Impact of selenium treatments on **d** shoot length; **e** root length; **f** shoot fresh weight and **g** root fresh weight under two concentrations of salt stress during the early seedling stage. Bars represent \pm SE of three replicates. The different letters indicate significant differences at $P < 0.05$ using Duncan's multiple range tests

(a)

Traits	FG %		GR		VI (I)		VI (II)	
	150 mM	200 mM	150 mM	200 mM	150 mM	200 mM	150 mM	200 mM
CK	96.33±0.88 ^{ab}	96.33±0.88 ^a	85.64±0.36 ^a	85.64±0.36 ^a	795.3±7.1 ^a	795.3±7.1 ^a	41.15±0.39 ^a	41.15±0.39 ^a
NaCl	94.33±0.88 ^{cd}	90.67±0.67 ^{de}	64.64±0.28 ^d	43.78±0.60 ^b	368.6±6.7 ^d	302.3±2.3 ^d	34.30±0.43 ^c	28.07±0.30 ^d
50 SeNPs	95.00±1.15 ^{bc}	92.00±1.15 ^{cd}	66.46±0.65 ^c	48.02±0.08 ^c	464.8±7.5 ^c	361.2±6.3 ^c	37.74±0.57 ^b	33.11±0.50 ^c
100 SeNPs	94.67±0.88 ^{bc}	92.67±0.88 ^{bc}	67.01±0.39 ^c	47.95±0.06 ^{cd}	242.9±2.1 ^e	216.4±3.8 ^e	33.23±0.31 ^c	29.03±0.90 ^d
150 SeNPs	95.33±0.88 ^{ab}	92.67±0.67 ^{bc}	66.98±0.38 ^c	51.68±0.55 ^b	461.0±3.1 ^c	368.8±1.5 ^c	38.41±0.31 ^b	33.66±0.37 ^c
50 Se (IV)	91.67±0.88 ^d	90.00±1.15 ^{de}	58.98±0.27 ^d	46.41±0.78 ^c	154.6±1.6 ^f	149.9±1.5 ^f	28.05±0.23 ^d	25.54±0.65 ^e
100 Se (IV)	97.33±0.67 ^a	94.00±0.58 ^b	69.06±0.63 ^b	52.18±0.29 ^b	541.0±5.8 ^b	395.8±8.0 ^b	41.17±0.31 ^a	35.75±0.57 ^b
150 Se (IV)	92.33±1.20 ^{cd}	89.00±0.58 ^d	58.10±0.37 ^d	43.33±0.81 ^b	138.5±1.9 ^f	137.5±4.3 ^f	25.43±0.34 ^d	22.06±0.42 ^f

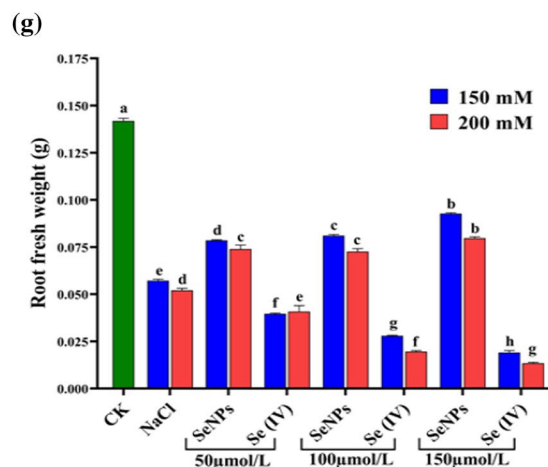
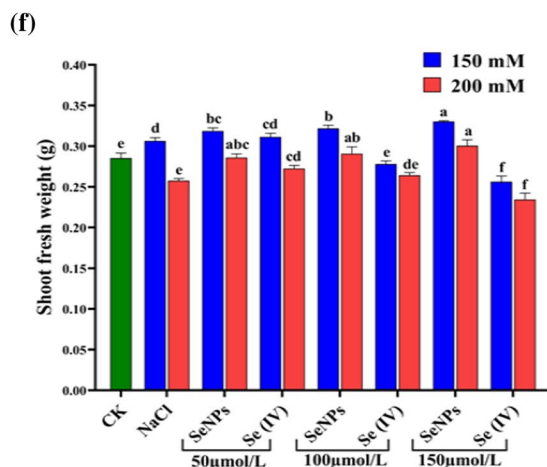
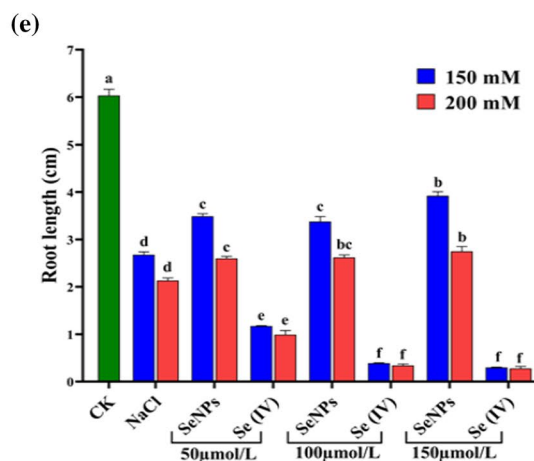
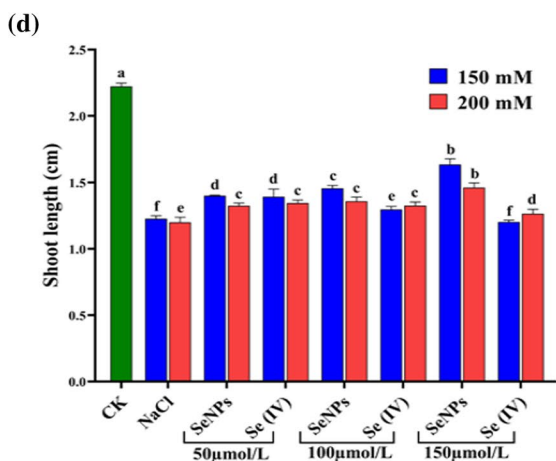
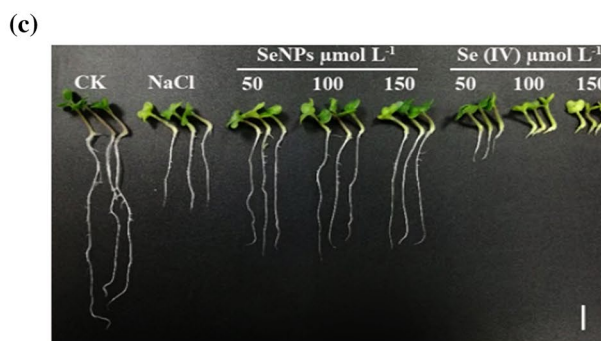
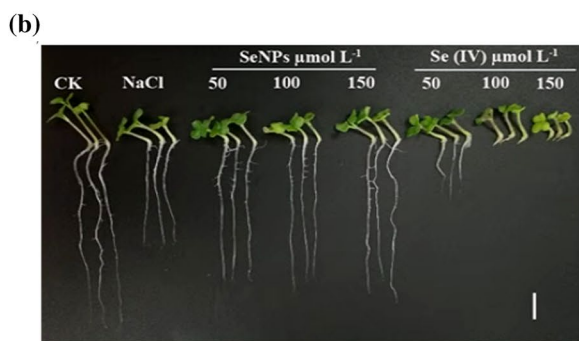


Fig. 6 (See legend on previous page.)

treated with NaCl alone (Fig. 6a). Furthermore, bioSeNPs alleviated the salinity stress and improved the FG% compared to Se (IV). Increasing salt stress levels on stressed plants without Se treatments significantly decreased the GR by 24.53 and 48.88% under 150 and 200 mM NaCl versus CK. While, bioSeNPs application with 50, 100 and 150 $\mu\text{mol L}^{-1}$ increased the GR by 2.81, 3.62 and 6.84% (150 mM), 9.69, 18.06 and 19.19% (200 mM) versus NaCl treated seedling alone. Besides this, Se (IV) strikingly 150 $\mu\text{mol L}^{-1}$ decreased the GR by 10.11 and 1.03% under 150 and 200 mM, respectively, compared to salinized seedlings without Se treatment (Fig. 6a). Finally, Se (IV) decrement was lower than NaCl seedlings but higher than bioSeNPs treatments.

Furthermore, VI (I) and VI (II) are significantly decreased in NaCl treated seedlings by 53.65 and 16.35% (150 mM), 60.39 and 32.02% (200 mM), respectively, versus CK. However, bioSeNPs treatments with 50, 100 and 150 $\mu\text{mol L}^{-1}$ increased the VI (I) by 26.07, 25.04 and 46.76% (150 mM), 19.50, 22.01 and 30.95% (200 mM), respectively, over NaCl treated seedlings alone. In contrast, Se (IV) decreased the VI (I) by 34.10, 58.06 and 62.42% (150 mM), 28.40, 50.41 and 54.51% (200 mM) under 50, 100 and 150 $\mu\text{mol L}^{-1}$ doses, respectively, versus NaCl. Besides, VI (II) increased by 20.04% (150 mM) and 27.34% (200 mM) with bioSeNPs (150 $\mu\text{mol L}^{-1}$), while Se (IV) decreased the VI (II) by 25.85% (150 mM) and 21.42% (200 mM) as compared to NaCl treated seedlings alone (Fig. 6a).

Impacts of Se treatments on growth parameters under two concentrations of NaCl

The impact of two forms of Se treatments on rapeseeds under salt stress during the early seedling stage were evaluated by examining their effect on phenotypic appearance traits and vegetative biomass. The application of bioSeNPs had the most promising effect on promoting rapeseed seedling growth versus Se (IV) and NaCl under 150 and 200 mM of NaCl (Fig. 6b, c).

A considerable 44.79 and 46.87% decreases in the shoot length were noticed under 150 and 200 mM NaCl, respectively, versus CK (Fig. 6d). However, bioSeNPs treatments with 50, 100 and 150 $\mu\text{mol L}^{-1}$ increased the shoot length by 14.10, 18.71 and 33.31% (150 mM), and 10.44, 13.22 and 21.81% (200 mM) over salinized seedlings alone (NaCl). Additionally, Se (IV) at 50 and 100 $\mu\text{mol L}^{-1}$ elevated the shoot length by 13.46 and 5.67% (150 mM) and 12.11 and 10.52% (200 mM). Meanwhile, 150 $\mu\text{mol L}^{-1}$ of Se (IV) decreased the shoot length by 1.99% under 150 mM but increased by 5.42% under 200 mM, compared to the seedlings treated with NaCl alone (Fig. 6d). With increasing the concentrations of

bioSeNPs, the shoot length increment was higher than NaCl and Se (IV) treated seedlings.

The root length inhibition under salt stress was recorded as 55.57 and 65.05% reduction under 150 and 200 mM NaCl versus CK, respectively (Fig. 6e). However, bioSeNPs treatments increased the root length by 30.29, 26.10 and 46.33% (150 mM), and 21.85, 22.85 and 28.81% (200 mM), additionally, Se (IV) decreased the root length by 56.19, 85.47 and 88.91% (150 mM), and 53.54, 84.06 and 86.91% (200 mM) with 50, 100 and 150 $\mu\text{mol L}^{-1}$ treatments, respectively, compared to the seedlings treated with NaCl alone, which suggested that Se (IV) highly negatively affected the seedlings comparing with NaCl and bioSeNPs treated seedlings (Fig. 6e).

The shoot fresh weight was increased under lower salt concentration 150 mM by 7.35%, while decreased by 9.73% under 200 mM comparison with CK. However, bioSeNPs treatments with 50, 100 and 150 $\mu\text{mol L}^{-1}$ significantly increased shoot fresh weight by 4.03, 5.05 and 7.80% (150 mM), and 10.98, 12.86 and 16.70% (200 mM), respectively, over CK. Additionally, Se (IV) treatments increased the shoot fresh weight by 1.61% (150 mM) and 5.79% (200 mM) at 50 $\mu\text{mol L}^{-1}$, while shoot fresh weight was decreased by 16.30% (150 mM) and 8.97% (200 mM) at 150 $\mu\text{mol L}^{-1}$, compared to NaCl treated seedlings (Fig. 6f). Seedlings grown under stressed conditions had lower root fresh weight than unstressed plants, which was decreased by 59.67 and 63.29% under 150 and 200 mM, respectively (Fig. 6g). However, under bioSeNPs treatments, the root fresh weight was increased versus salt-stressed seedlings alone (NaCl) by 33.37, 41.77 and 62.10% (150 mM), and 42.20, 39.52 and 53.10% (200 mM), while Se (IV) significantly reduced the root fresh weight by 30.68, 51.14 and 66.71% (150 mM), and 21.64, 62.44 and 74.29% (200 mM) under 50, 100 and 150 $\mu\text{mol L}^{-1}$, respectively, versus stressed plants alone (Fig. 6g).

Impacts of Se treatments on photosynthetic pigments under two concentrations of NaCl

The results indicated significant differences ($P < 0.05$) between the treatments and photosynthetic pigments. Salinity induced negative impacts on photosynthetic pigments, which reduced total chlorophyll, chlorophyll a, chlorophyll b and carotenoids contents by 27.19, 24.48, 30.25 and 45.13% (150 mM), and 34.73, 29.83, 39.93 and 51.54% (200 mM), respectively, versus CK seedlings (Table 1). Moreover, the chlorophyll contents were affected by Se application in both forms, especially 150 $\mu\text{mol L}^{-1}$ of bioSeNPs and Se (IV), which increased by 65.09 and 5.63% (chlorophyll a), 64.57 and 14.60% (chlorophyll b), 64.85 and 9.81% (total chlorophyll) under 150 mM, while 67.25 and 25.04% (chlorophyll a), 83.22

Table 1 Impacts of selenium treatments on photosynthetic pigments (mg g⁻¹ FW) under two concentrations of salt stress during the early seedling stage

Traits	Chlorophyll a		Chlorophyll b		Total chlorophyll		Carotenoids		
	150 mM	200 mM	150 mM	200 mM	150 mM	200 mM	150 mM	200 mM	
CK	3.628 ± 0.07 ^c	3.628 ± 0.07 ^b	3.428 ± 0.05 ^b	3.428 ± 0.05 ^b	7.056 ± 0.11 ^c	7.056 ± 0.11 ^b	22.29 ± 0.27 ^a	22.29 ± 0.27 ^a	
NaCl	2.746 ± 0.08 ^f	2.546 ± 0.08 ^d	2.391 ± 0.05 ^e	2.059 ± 0.07 ^e	5.137 ± 0.08 ^g	4.605 ± 0.15 ^e	12.23 ± 0.49 ^f	10.80 ± 0.30 ^f	
50 μmol L ⁻¹	SeNPs	3.528 ± 0.08 ^c	3.258 ± 0.09 ^c	3.088 ± 0.10 ^c	2.978 ± 0.07 ^{cd}	6.616 ± 0.02 ^d	6.236 ± 0.16 ^{cd}	18.79 ± 0.40 ^{cd}	17.74 ± 0.33 ^{cd}
	Se (IV)	3.025 ± 0.03 ^{de}	3.285 ± 0.06 ^c	2.864 ± 0.08 ^{cd}	3.117 ± 0.03 ^c	5.888 ± 0.09 ^{ef}	6.402 ± 0.07 ^c	19.82 ± 0.20 ^c	18.29 ± 0.54 ^{cd}
100 μmol L ⁻¹	SeNPs	4.075 ± 0.05 ^b	3.748 ± 0.08 ^b	3.726 ± 0.07 ^a	3.545 ± 0.09 ^b	7.801 ± 0.06 ^b	7.293 ± 0.08 ^b	19.84 ± 0.18 ^c	18.71 ± 0.31 ^c
	Se (IV)	3.153 ± 0.04 ^d	3.316 ± 0.06 ^c	2.971 ± 0.09 ^c	2.981 ± 0.09 ^{cd}	6.124 ± 0.10 ^e	6.297 ± 0.03 ^{cd}	18.57 ± 0.34 ^d	17.29 ± 0.54 ^{de}
150 μmol L ⁻¹	SeNPs	4.533 ± 0.08 ^a	4.258 ± 0.15 ^a	3.935 ± 0.05 ^a	3.773 ± 0.05 ^a	8.468 ± 0.11 ^a	8.031 ± 0.18 ^a	21.05 ± 0.28 ^b	20.57 ± 0.30 ^b
	Se (IV)	2.900 ± 0.09 ^{ef}	3.183 ± 0.06 ^c	2.741 ± 0.10 ^d	2.851 ± 0.09 ^d	5.641 ± 0.05 ^f	6.034 ± 0.10 ^d	17.48 ± 0.55 ^e	16.68 ± 0.25 ^e

Data presented are the mean ± SE of three replicates. The different letters indicate significant differences at $P < 0.05$ using Duncan's multiple range tests

and 38.44% (chlorophyll b), 74.40 and 31.03% (total chlorophyll) under 200 mM, respectively, versus NaCl treated seedlings. On the other hand, carotenoids content was increased by 72.17 and 42.99% (150 mM), 90.52 and 54.48% (200 mM) with 150 μmol L⁻¹ of bioSeNPs and Se (IV), respectively over NaCl treated seedlings (Table 1).

Impacts of Se treatments on osmoprotectants and MDA content under two concentrations of NaCl

Upon exposure to 150 and 200 mM, 80.08 and 111.2%, significantly higher total soluble sugar (TSS) content has been seen, respectively, over CK in NaCl treated seedlings. Moreover, TSS content was affected by bioSeNPs and Se (IV) application, especially 150 μmol L⁻¹, which decreased TSS content by 19.86 and 9.38% (150 mM), 35.28 and 16.48% (200 mM), respectively, versus NaCl treated seedlings alone without Se treatments (Fig. 7a).

Compared with CK, total soluble protein (TSP) content was increased in NaCl treated seedlings by 55.67 and 142.6% under 150 and 200 mM, respectively. The Se treatments remarkably decreased TSP content by 33.84, 29.67 and 21.35% (150 mM), and 17.69, 16.43 and 10.01% (200 mM) with bioSeNPs, 13.48, 6.14 and 3.75% (150 mM), and 13.64, 4.73 and 2.85% (200 mM) with Se (IV) at 50, 100 and 150 μmol L⁻¹, respectively, versus NaCl treated seedlings (Fig. 7b).

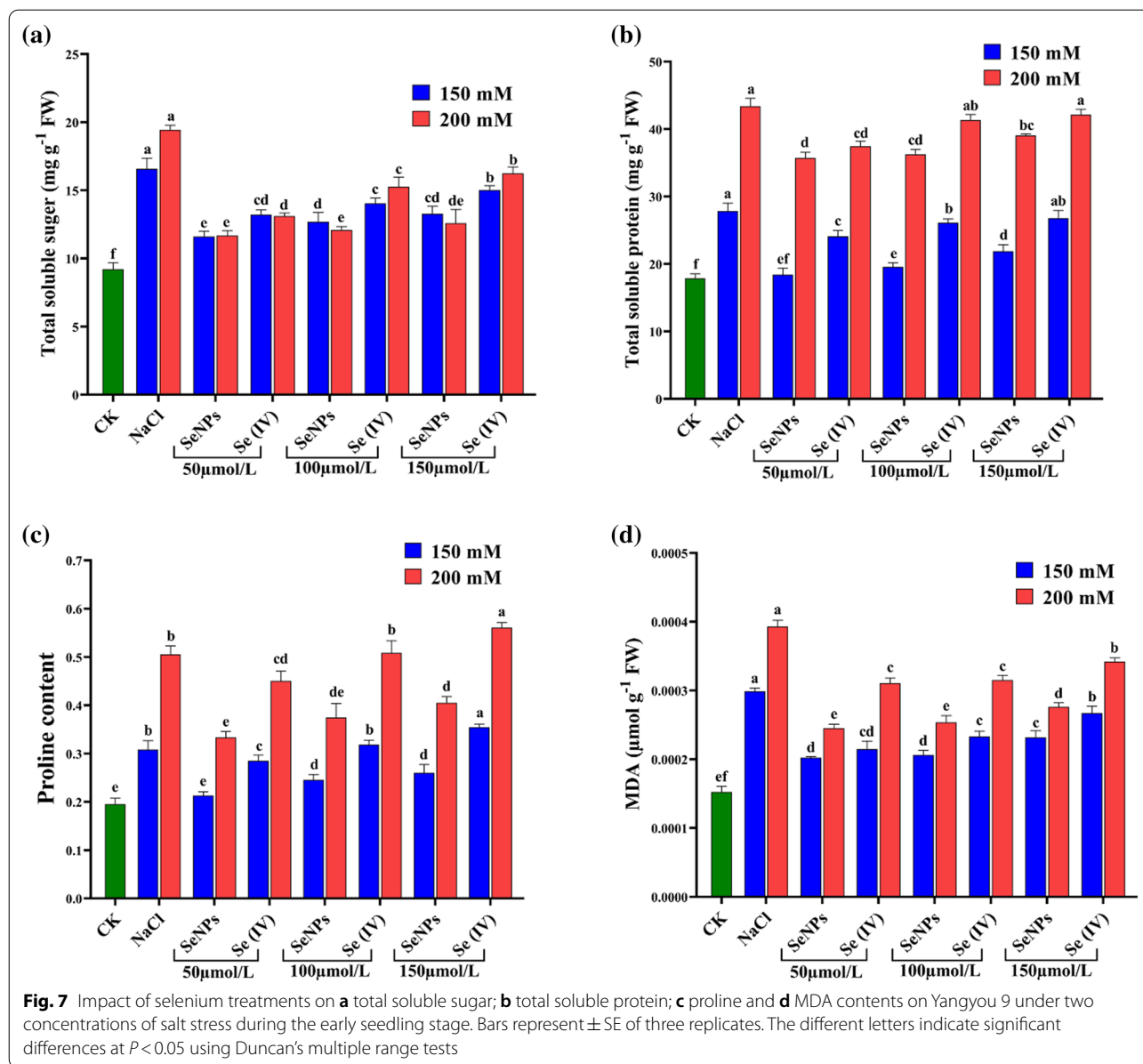
Proline content significantly increased by 57.86 and 158.6% under 150 and 200 mM of NaCl without Se application versus CK. Compared with NaCl treated seedlings alone without Se treatments, 150 μmol L⁻¹ of bioSeNPs treatment decreased proline content by 15.78% (150 mM) and 19.78% (200 mM), while 150 μmol L⁻¹ of Se (IV) treatment increased proline content by 15.02% (150 mM) and 10.94% (200 mM) (Fig. 7c).

Lipid peroxidation was determined to assess cell membrane integrity related to oxidative damage. For this

purpose, the MDA level was analyzed that showed significant differences in lipid peroxidation among all treatments. Seed's exposure of 150 and 200 mM without Se treatments extensively elevated the MDA level versus CK showed a maximum upsurge by 95.93 and 157.5%, respectively. Additionally, 150 μmol L⁻¹ of Se increased MDA content by 51.70 and 75.15% (150 mM), 80.82 and 124.2% (200 mM) on bioSeNPs and Se (IV), respectively, over CK. Meanwhile, MDA content was decreased by 22.58 and 10.60% (150 mM), 29.78 and 12.91% (200 mM) with 150 μmol L⁻¹ of bioSeNPs and Se (IV), respectively, compared to the seedling treated with NaCl alone (Fig. 7d). Besides, bioSeNPs treatments showed lower MDA content than Se (IV) treatments under salt stress.

Impacts of Se supplementation on Na⁺, K⁺ and Na⁺/K⁺ ratio in shoots under two concentrations of NaCl

Se application decreased the Na⁺ level in the shoots and significantly elevated the uptake of K⁺ (Table 2). Under stress conditions, the Na⁺/K⁺ ratio in NaCl shoots (without Se treatments) was increased by 34.57% (150 mM) and 18.40% (200 mM) as compared to CK. Meanwhile, supplementation of Se (both forms) decreased the Na⁺ uptake and Na⁺/K⁺ ratio as well as increased the K⁺ uptake, especially, 150 μmol L⁻¹ of bioSeNPs and Se (IV), which decreased the Na⁺ content by 35.29 and 26.88% (150 mM), 34.64 and 24.34% (200 mM), and increased the K⁺ content by 203.3 and 136.7% (150 mM), 414.2 and 233.6% (200 mM), as well as reduced the Na⁺/K⁺ ratio by 78.66 and 69.10% (150 mM), 87.92 and 77.32% (200 mM), respectively, versus NaCl. Ultimately, bioSeNPs showed significant positive effects strikingly stronger on the mineral uptake (Table 2).



BioSeNPs and Se (VI) affected Se pathway-related genes in *B. napus* root tissues under 150 μmol L⁻¹

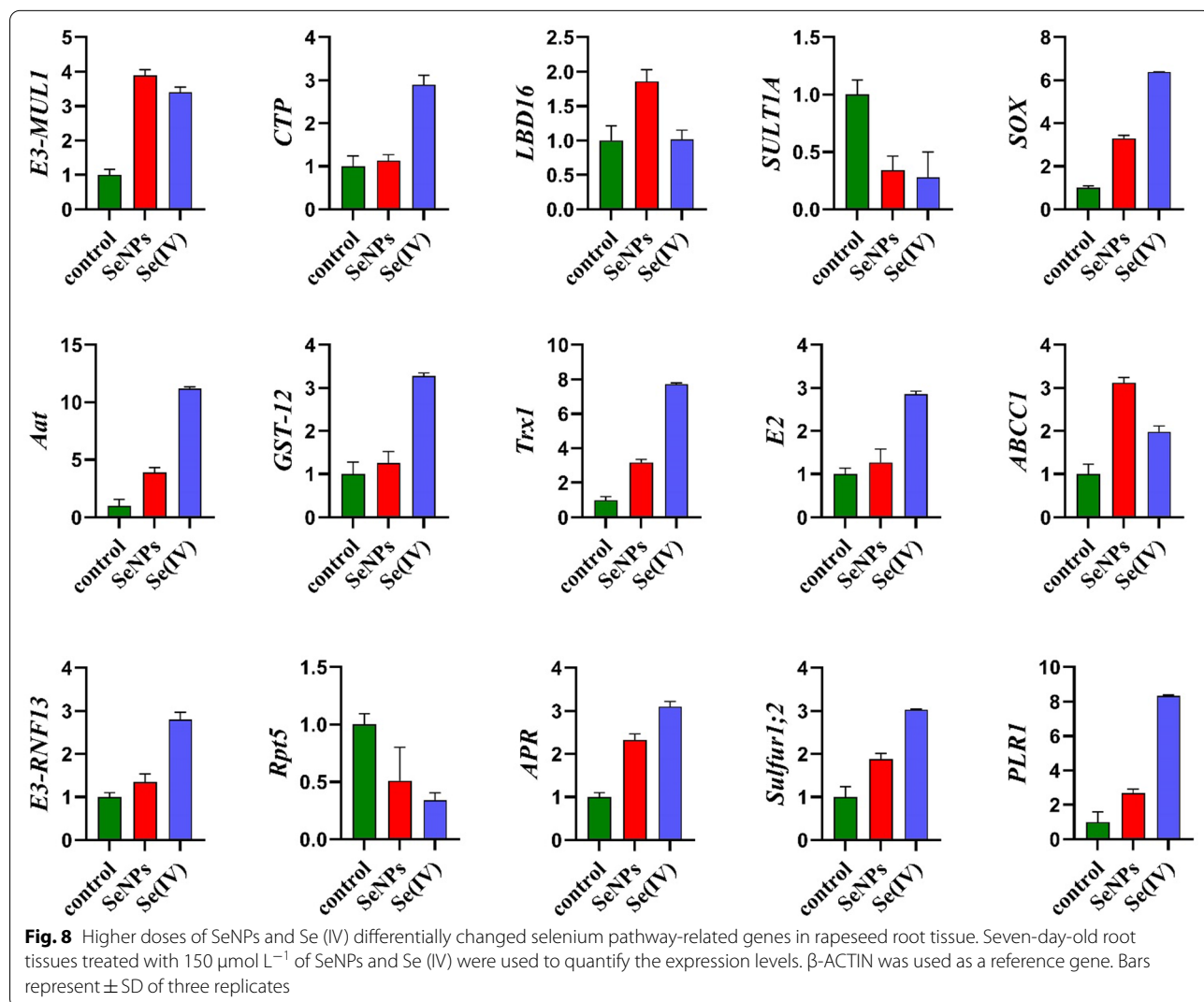
The transcription levels of Se pathway-related genes were determined to evaluate the impact of bioSeNPs and Se (IV) on root tissues of *B. napus*. In seedlings-root, the expression of sulfite oxidase gene (*SOX*) was up-regulated under bioSeNPs and Se (IV) treatments by 3.30 and 6.39-fold, respectively (Fig. 8). Our results verified that Se (IV) could transform into Se (VI) form, which persists in the metabolic pathway. Also, the storage function of the vacuole is of great importance, which was verified through genes upregulation in the metabolism.

Also, Se (IV) stress enhanced the gene expression of both *Aat* and *PLR1* by 11.19 and 8.33-fold, respectively, which are significant genes for the metabolism of amino acids, and might participate in the determination of the pyridoxal phosphate content in the cell. Meanwhile, bioSeNPs treatment induced the expression of *LBD16* by a 1.86-fold relative to control (Fig. 8). Our findings illustrated that bioSeNPs could improve lateral root production in plants, one of the main architectural determinants for root development. Previously NPs were well documented to have essential functions in growth by increasing the expression of *LBD16*, which acts downstream of the auxin influx carriers *AUX1* and *LAX1* in

Table 2 Impact of selenium supplementation on Na⁺, K⁺ and Na⁺/K⁺ ratio in shoots under two concentrations of salt stress during the early seedling stage

Traits	Na ⁺ mg/g		K ⁺ mg/g		Na ⁺ /K ⁺	
Treatments	150 mM	200 mM	150 mM	200 mM	150 mM	200 mM
CK	3.80 ± 0.33 ^e	3.80 ± 0.33 ^f	7.77 ± 0.17 ^f	7.77 ± 0.17 ^f	0.49 ± 0.04 ^b	0.49 ± 0.04 ^b
NaCl	36.47 ± 0.65 ^a	46.76 ± 0.71 ^a	2.37 ± 0.29 ^e	0.98 ± 0.59 ^e	15.39 ± 0.01 ^a	47.71 ± 0.26 ^a
50 μmol L ⁻¹	SeNPs 26.25 ± 0.52 ^c	35.23 ± 0.28 ^c	5.02 ± 0.59 ^c	2.83 ± 0.35 ^b	5.23 ± 0.21 ^{def}	12.45 ± 0.12 ^{de}
	Se (IV) 30.57 ± 0.32 ^b	36.54 ± 0.26 ^c	3.33 ± 0.64 ^d	2.01 ± 0.68 ^d	9.18 ± 0.22 ^c	18.18 ± 0.15 ^c
100 μmol L ⁻¹	SeNPs 25.22 ± 0.57 ^{cd}	32.47 ± 0.91 ^d	5.56 ± 0.58 ^b	3.68 ± 0.08 ^b	4.54 ± 0.31 ^{ef}	8.820 ± 0.19 ^{ef}
	Se (IV) 29.34 ± 0.71 ^b	38.23 ± 0.35 ^b	4.04 ± 0.54 ^d	2.52 ± 0.68 ^c	7.26 ± 0.44 ^{cd}	15.17 ± 0.35 ^{cd}
150 μmol L ⁻¹	SeNPs 23.60 ± 0.61 ^d	30.56 ± 0.55 ^e	7.19 ± 0.49 ^a	5.04 ± 0.70 ^a	3.28 ± 0.32 ^f	6.060 ± 0.19 ^f
	Se (IV) 26.67 ± 0.93 ^c	35.38 ± 0.39 ^c	5.61 ± 0.62 ^c	3.27 ± 0.33 ^b	4.75 ± 0.21 ^{de}	10.82 ± 0.27 ^{de}

Data presented are the mean ± SE of three replicates. The different letters indicate significant differences at P < 0.05 using Duncan's multiple range tests



the regulation of lateral root initiation and development; thus, it regulates the developmental processes in plants [49].

Mitochondrial located gene *E3* ubiquitin-protein ligase *MUL1* was highly expressed along with *E3-RNF13* and ubiquitin-conjugating enzyme *E2* genes, which are important for the ubiquitin-proteasome pathway (UPP). Furthermore, sulfate transporter 1;2 (*Sultr1;2*) is an essential protein for sulfate and selenate transportation, which is increased by 1.88 and 3.03-fold under bioSeNPs and Se (IV) treatments, respectively, which in turn played an important role in selenium uptake repression. The expression level of *APR1* recorded 2.33 and 3.10-fold, while the expression level of *SULT1A* decreased by 0.34 and 0.28-fold under bioSeNPs and Se (IV), respectively (Fig. 8).

BioSeNPs and Se (IV) up-regulated the expression level of *Trx 1* by 3.18 and 7.72-fold, respectively (Fig. 8), which

played significant roles in detoxifying ROS and the maintenance of cellular redox homeostasis via structural alterations of target proteins [50]. Consequently, the Se (IV) treatments negatively affected the root growth of rapeseed seedlings versus bioSeNPs and relative control.

Effect of bioSeNPs and Se (VI) on Se pathway-related genes in *B. napus* shoot tissues under 150 $\mu\text{mol L}^{-1}$

To explore the impact of bioSeNPs and Se (IV) on Se pathway-related genes in *B. napus* shoot tissue, we have selected *ABCC2* from the C subfamily of the ATP-binding cassette transporters (ABCC) and *GST-u4* from the glutathione S-transferase family, which was increased by 1.28- and 1.71-fold under bioSeNPs treatment and 1.60 and 2.28-fold under Se (IV) treatment, respectively. Furthermore, Se (IV) treatment increased the expression levels of *CyS*, *MET*, and *CBL* by 1.83, 2.03 and 1.30-fold, respectively. These three enzymes are

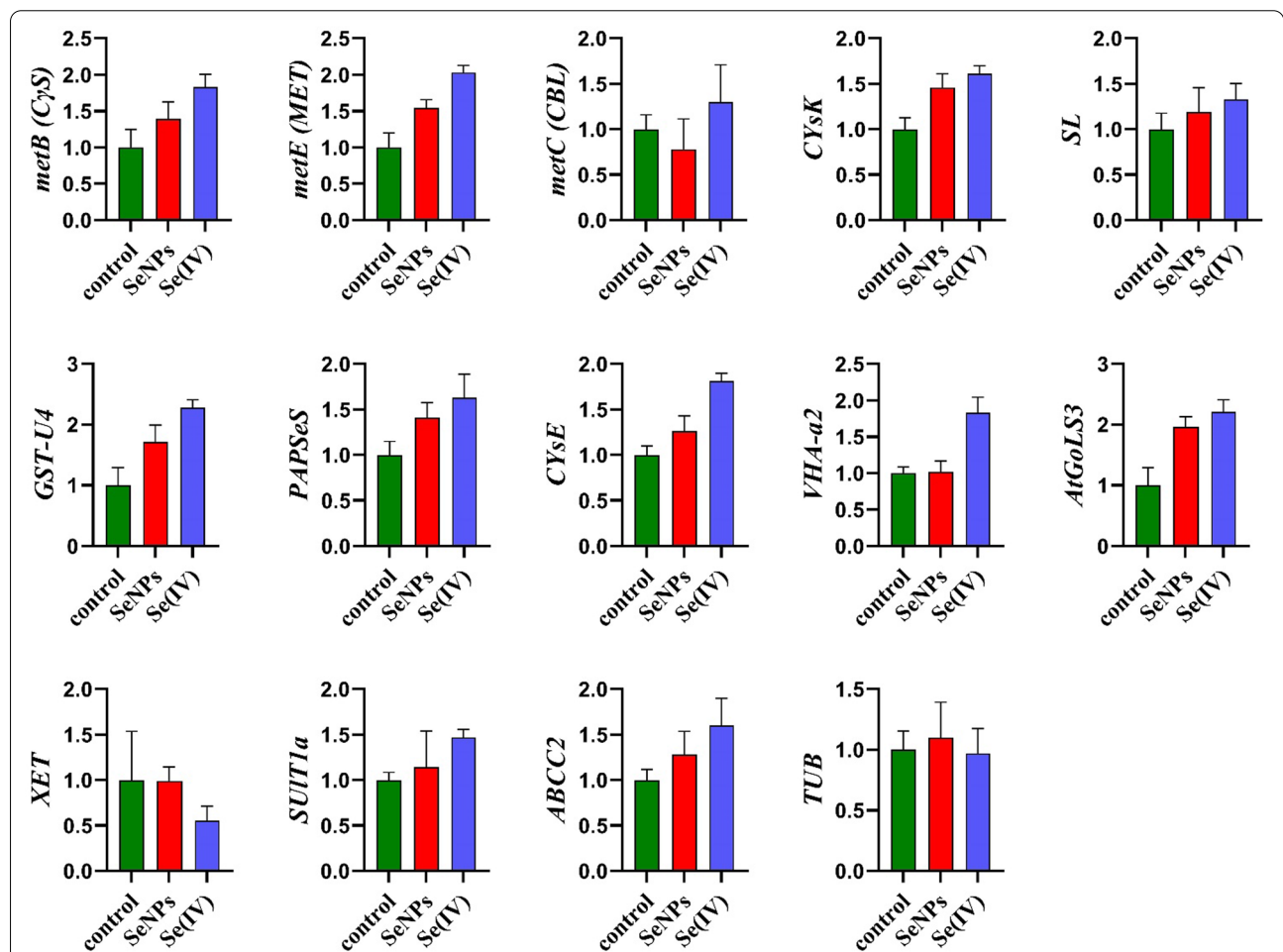


Fig. 9 Higher doses of SeNPs and Se (IV) differentially changed selenium pathway-related genes in rapeseed shoot tissues. Seven-day-old shoot tissues treated with 150 $\mu\text{mol L}^{-1}$ of SeNPs and Se (IV) were used to quantify the expression levels. β -ACTIN was used as a reference gene. Bars represent \pm SD of three replicates

critical in the methionine biosynthetic pathway (Fig. 9). Meanwhile, *CysK*, *CysE* and *SL* increased under Se treatments by 1.46, 1.26 and 1.19-fold (bioSeNPs), 1.61, 1.81 and 1.33-fold (Se (IV)), respectively.

SULT1A is a member of the sulfotransferase (SOT) protein family, which significantly participates in the selenation pathway [51]. The transcription level of *SULT1A* was increased by 1.14-fold (bioSeNPs) and 1.47-fold (Se (IV) in the shoot tissues (Fig. 9). *AtGoLS3* belongs to the galactinol synthase (*GoLS*) family is a key regulator in raffinose family oligosaccharides (RFOs) synthesis that promotes plant stress tolerance under various abiotic stresses [52]. Regarding our results, the *AtGoLS3* gene expression under selenium treatments was increased by 1.96 and 2.21-fold under bioSeNPs and Se (IV), respectively (Fig. 9). These results suggested that *AtGoLS3* was enhanced under abiotic and metal stress.

However, the expression level of *XET* was reduced by 0.55-fold under Se (IV), while slightly reduced under bioSeNPs treatments (0.55-fold), it contributed to the wall stress relaxation, strengthening, gravitropism and increased the creep of cellulose xyloglucan composites in the cell wall during biosynthesis [53]. The existing gene on mature phagosomes *VHA-a2* was enhanced by 1.02- and 1.83-fold in the shoot tissues under bioSeNPs and Se (IV) treatments, respectively. At the same time, the changes in the expression level of *TUB* gene increased by 1.10- and 0.97-fold at bioSeNPs and Se (IV), respectively (Fig. 9).

Discussion

Nanoparticles including metallic elements such as CuNPs, FeNPs, CeNPs, TiNPs, AgNPs and ZnNPs interact with plant cells at the physicochemical level based on their surface properties, giving each element a typical response by enhancing the uptake of beneficial or essential elements to the plant [54–56]. Nowadays, SeNPs has attracted many researchers, owing to their unique physicochemical properties and availability, which increased the application of Se in the agricultural field, particularly under biotic and abiotic stresses. Our goal is to investigate the effect of two forms of Se (bioSeNPs and Se (IV)) on germination and growth under normal and salt stress conditions using higher Se doses in *B. napus*.

BioSeNPs positively affect seed germination and seedling growth of *B. napus* during the early seedling stage

In our study, bioSeNPs possess lower phytotoxicity than Se (IV) in seedlings under normal and salt stress conditions. It may significantly affect plant development and seed germination, which impact seedling growth under higher Se doses. This result indicated that the application

of bioSeNPs induced marked proliferation in growth parameters. Furthermore, it was reported that plants can easily uptake and transport NPs [57], suggesting that bioSeNPs might be interacting with plants at the cellular and subcellular levels after entering the plant cell and promoting changes in morpho-physicochemical attributes [58, 59].

Moreover, SeNPs positively impacted several physicochemical mechanisms and improved shoot and root development in tomato plants [48], encouraging organ production and root development in tobacco [60]. These studies, as mentioned earlier, could explain our findings of bioSeNPs enhancing the seedling growth and biomass, which was observed in comparison with Se (IV).

Contrarily, Se (IV), especially 150 $\mu\text{mol L}^{-1}$, declined the growth traits under both conditions (normal and salt stress conditions), which caused chlorosis and stunted plant growth, leaves withering, dryness and premature death [61, 62]. Moreover, higher doses of Se (IV) induced adverse effects on seedling development, which increased ROS accumulation, deterioration in total chlorophyll contents, and un-specified substitution of sulfate ion (SO_4^{2-}) in S-containing substances and protein that inhibited the growth parameters [63, 64].

Nano-Se positively affect the photosynthetic pigments and osmolality components

Photosynthetic pigments are essential energy sources of plant biological systems, which are a vital index of photosynthesis and any alteration causes a parallel effect on metabolism [57]. Interestingly, in our study, bioSeNPs significantly increased the chlorophyll contents compared to Se (IV) and untreated seedlings (Control) under normal and stress conditions. We noticed that 150 $\mu\text{mol L}^{-1}$ showed the highest value of chlorophyll contents due to higher protection of photosynthetic pigments with higher Se concentration. However, bioSeNPs 50 and 100 $\mu\text{mol L}^{-1}$ showed a non-significant difference compared to each other. Furthermore, previous studies reported that the effect of NPs on the chlorophyll contents is concentration-dependent [54, 65, 66]. Therefore, different concentrations of NPs are of great importance for the various effects on plant's physiological processes [67]. A higher chlorophyll contents might be related to bioSeNPs induced protection of certain chloroplast enzymes by improving antioxidant enzymatic capacity [68]. Se plays a role as the catalytic center of selenoproteins like GPx and scavenges the free radicals that protect the photosynthetic pigment [2]. On the other side, higher doses of Se (IV) declined the chlorophyll contents, which may induce some oxidative strain and lead to peroxidation of chloroplast membrane and photosynthetic degeneration [69]. Additionally, the higher concentration of Se

resulted in a lower photosynthetic capacity, presumably attributable to the chlorophyll degeneration induced by the decrease in carotenoids [70, 71].

Osmolytes are essential to improve the defense system under different stresses, supplying metabolites and energy via several physiochemical operations [72]. Bio-SeNPs improve osmotic substances through osmotic potential maintenance within the cytoplasm and vacuoles during the metabolic processes and provide cellular protection against ROS accumulation. In general, the metallic NPs may improve the light absorption through chloroplast by increasing the gene expression response to light-harvesting complex II, raising the osmolyte contents [73, 74].

Additionally, the plant growth performance is mainly correlated with the water status. The plant responds to water shortage by accumulating several osmotic protectants such as proline [75, 76]. In this investigation, we noticed a dramatic elevation in proline contents under Se (IV) than bioSeNPs, which may explain the exceptional ability of rapeseed seedlings to resist selenium-induced water loss; moreover, higher proline content indicated stress level [77]. Generally, bioSeNPs non-significantly affected the proline content under both conditions, which explained the critical role of proline in plants to avoid the harmful effects of ROS [78].

BioSeNPs induced plant defense system under normal and stress conditions

Malondialdehyde (MDA) is produced by the oxidative degradation of cellular membrane, an indicator of membrane damage, considered another parameter reflecting the cell's vitality [20]. In the current study, the MDA content was increased in treated seedlings with Se (IV), which may cause specific stress and thus induce enzymatic and non-enzymatic antioxidants [77, 79]. In contrast, bioSeNPs recorded a slight increment in MDA content over the relative control because of the specific response of rapeseed seedlings to nano-Se by improving photosynthesis besides antioxidant enzyme activity.

ROS leads to oxidative stress and disrupts various cellular structures in plants [80]. The equilibrium between production and scavenging of ROS decides either oxidative damage or stress signalling [1], and the excessive ROS production is responsible for substituting sulfur, preventing methylation and Se-toxicity [2]. Furthermore, SOD and CAT activities were not synchronized due to the continuous elevation of SOD and the reduction of CAT activities, which accelerated the generation of H_2O_2 under Se treatments in rapeseed seedlings, especially under Se (IV) compared to bioSeNPs. Besides, bioSeNPs affected antioxidant enzymes efficiencies, thus protecting the plants and enhancing the growth, which indicated the free

radicle detoxification [81–83], antioxidant defense system stimulation and ROS quenching by NPs [57]. Meanwhile, Se (IV) toxicity was potentiated by impairment of oxidative metabolism and higher productions of ROS, as evidenced by higher accumulation of H_2O_2 , $O_2^{\bullet-}$ and lipid peroxidation that caused plasma membrane injury [70].

Our investigation showed that bioSeNPs application-maintained homeostasis in the cell by inducing the gene expression of antioxidant enzymes related genes owing to higher POX activity. The following activities of SOD and CAT lessened the ROS damage by $O_2^{\bullet-} \rightarrow H_2O_2 \rightarrow H_2O$ progression due to the protective role of Se under oxidative stress [84, 85], suggesting that nano-treatment can alleviate oxidative damages of metal toxicity and salt stress by decreasing the excessive lipid peroxidation, which improves cellular integrity. Contrarily, a higher dose of Se (IV) influenced the transcription level and activity of antioxidant enzymes by promoting SOD and reducing CAT activities, ultimately excessive ROS accumulation [70].

Supplementation of bioSeNPs reduced the Na^+ toxicity during the early seedling stage

A plant's ability to maintain both K^+ and Na^+ homeostasis is an essential trait indicating its salinity stress tolerance. Massive over-accumulation of Na^+ in the cytosol leads to Na^+ toxicity and causes K^+ efflux from the cytosol to apoplast. BioSeNPs application increased K^+ level with reduction of Na^+ level under two concentrations of NaCl (150 and 200 mM) during the early seedling stage, which promotes the regulation of growth by inference to antioxidant metabolism and cellular stress signalling [86]. It could be concluded that the enhancement in rapeseed growth, total chlorophyll and mineral contents of seedlings exposed to salt conditions with bio-SeNPs application may be due to reducing Na^+ content in leaves, consequently reducing Na^+/K^+ ratio, osmotic adjustment, ionic balance and antioxidant enzyme activities [87]. NPs elevate the expression of Na^+/H^+ antiport and tonoplast H^+ -ATPase at the root membranes and shorten the root apoplast barrier, thus limiting Na^+ translocation to shoot tissues and reducing Na^+ toxic effects [88, 89], hence improving salt tolerance. Se application alleviates salinity stress by enhancing PSII function and decreasing Na^+ content in the shoot via binding of Na^+ to the root cell wall, ultimately reducing the accumulation of Na^+ ions in plant organs [90].

K^+ is a co-factor required to activate more than 50 enzymes [91] and plays a vital role in cytosolic pH homeostasis, protein synthesis and cell activities, including stomatal opening and closure [92]. Conclusively, we found that bioSeNPs treated seedlings showed a better ability to maintain total leaf K^+ content than Se (IV) under salt stress. These results confirmed that bioSeNPs helped

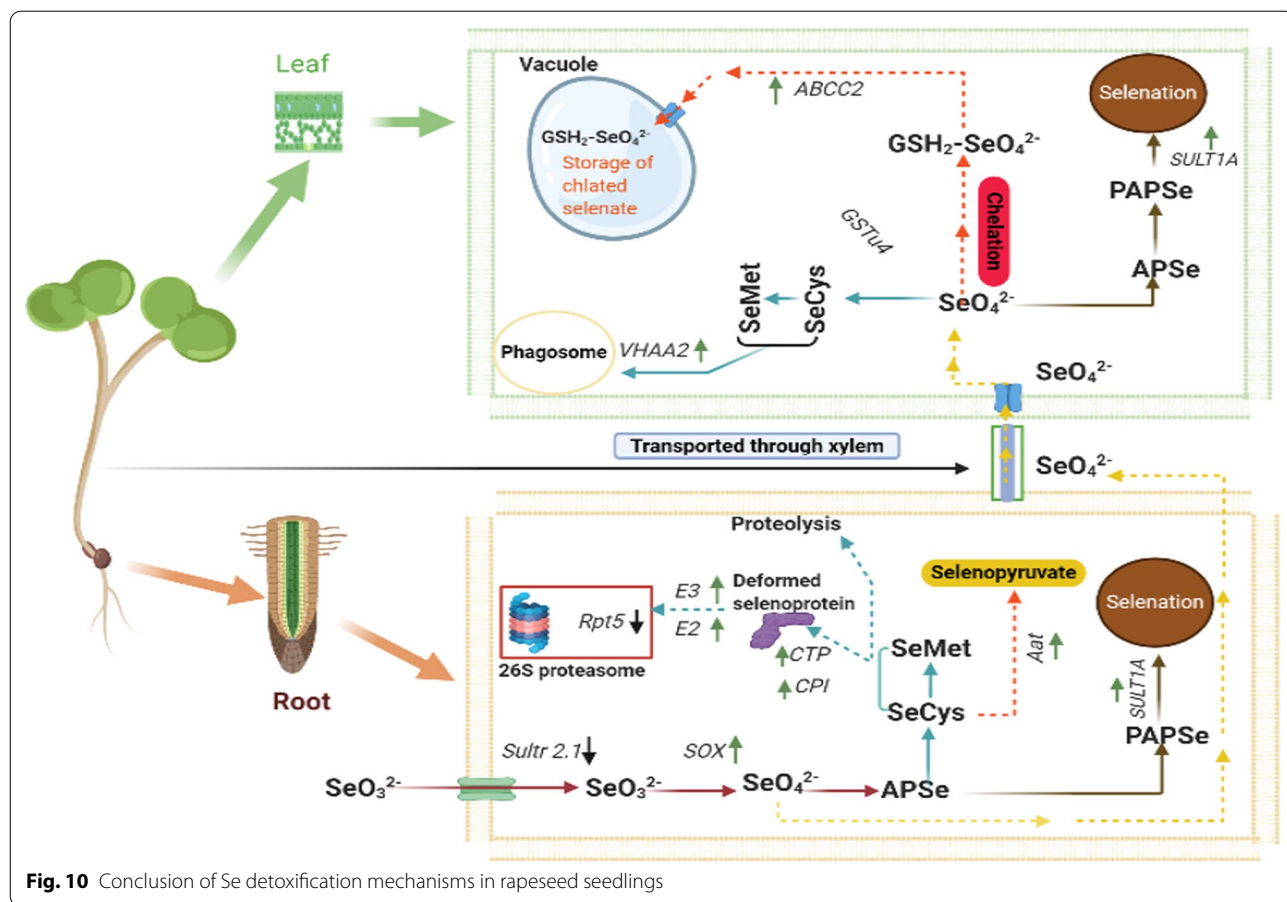


Fig. 10 Conclusion of Se detoxification mechanisms in rapeseed seedlings

rapeseed seedlings to maintain a better leaf Na^+/K^+ ratio, thus better performance under salinity stress. Overall, this work suggests that retaining the leaf Na^+/K^+ ratio is a component of the mechanisms behind SeNPs enabled better plant salt tolerance.

Se (VI) as a fundamental compound in the Se pathway

Most of the plants nonspecifically uptake selenate using sulfate transporters as Se, which is similar to S in terms of its chemical characteristics [93, 94]. To convert Se (VI) into Se (IV), the performance of both APS and APR enzymes is essential. APS enzyme intercedes the Se (VI) linkage with ATP, resulting in adenosine phosphoselenate (APSe), which is converted into Se (IV) via APR [6]. Furthermore, the rise in SOX level confirmed that Se (IV) might be transformed into Se (VI), then integrated to ATP through APS, converted to Se (IV) through APR, then into selenide; finally, integrated into SeCys in rapeseed seedlings specifically in root tissues (Fig. 10).

Vacuole plays a vital role under high doses of Se

The formation of APSe, followed by the increase of GST-u4, facilitated the transformation of Se (VI) to

GSH and glutathione-S conjugate (GS-X). The subfamily C-CFTR/MRP of the ATP-binding cassette superfamily was first identified as phytochelatin transporters in the sequestration of toxic elements in the vacuole [95, 96]. Therefore, we deduced that glutathione-derived peptides partially chelated Se (VI) with glutathione sulfurtransferase (GST), then translocated to the vacuole through MRP2 to protect the cell from the deleterious Se effects and Se sequestration in different tissues (shoot and root). Our findings proposed that vacuole storage functions are vital to cope with high concentrations of Se in *B. napus* seedlings (Fig. 10).

Transamination plays a significant role to protect plant cells against Se toxicity

SeCys is one of the critical factors for Se toxicity, and the misincorporation of SeCys affects the Se-detoxification ability of plants [97]. SeCys methyltransferase is the main factor in SeCys methylation, using CyS to rehabilitate into SeMet, and it is specifically degraded or oxidized through *CpNifS* and *SL*, respectively [6]. Our results confirmed that the up-regulation of *CyS*, *CBL* and *MET* is responsible for SeCys-SeMet conversion in the shoot tissues. While, the

higher expression levels of *PLR1* and *Aat* in the root tissues are also located in the cysteine and methionine metabolic pathway [98], which concluded SeCys deamination by *Aat* as a remarkable way for Se tolerance (Fig. 10).

Selenation is a substantial way for Se detoxification

Selenation is one of the most important pathways for Se detoxification, similar to the sulfation process that can reduce SeCys biosynthesis. On the other side, *APR* is considered a critical enzyme for reducing selenate and sulfate [2]. Furthermore, our observation suggested that the Se (VI) either chelated by *GSH* then entered in the vacuole or shifted to a phenolic hydroxy group by *APSe*, *PAPSeS* and *SULT1A*, ultimately formed selenocompound substrates [51]. Our conclusion reported that the selenation process also happened at high selenium doses in the root tissues. The selenation activity was greater in shoots than roots due to the higher expression level of *SULT1a* under Se toxicity. Correspondingly, our results supported that selenation is a more functional method of Se detoxification in rapeseed seedlings (Fig. 10).

Selenoproteins degradation is a noteworthy pathway for Se detoxification

The SeMet and SeCys are selenoamino acids that might be misincorporated with proteins. Cysteine occupies an essential position in structural integrity and functional maintenance of protein. Moreover, it contributes to various processes such as enzymatic reactions, redox homeostasis, folding of the protein and metal detoxification. Protein deformation probably occurs by substituting SeCys in non-specific selenoproteins, leading to diselenide linkage or a mixed selenide-sulfide linkage, which are different in characteristics. Therefore, the non-specific SeMet accumulation is reported as less detrimental than highly reactive SeCys [64]. Chaperone-mediated processes induced the formation of deformed or malformed selenoproteins, and the proteolysis of irreparable proteins through the lysosome or the ubiquitin–proteasome pathway (UPP) can also occur. The processes of nullifying the production of selenoproteins are associated with Se tolerance in plants, which supports our findings [97, 99]. The changes in the expression levels of *E3* ubiquitin-protein ligase *MUL1*, *E2* ubiquitin-conjugating enzyme *RNF13* and cysteine-type peptidase in rapeseed roots, and *VHA-a2* in rapeseed shoots, in addition to the changes in *Rpt5* as an essential subunit for assembly of the 26S proteasome, indicate that the selenoproteins disintegration is a crucial way for Se tolerance, which is rhythmic with [97, 99, 100] (Fig. 10).

Conclusion

We aimed to investigate the effect of bioSeNPs and Se (IV) on morpho-physiochemical attributes under normal and salt stress conditions, besides the molecular mechanisms and genes involved in Se detoxification during the early seedling stage. Our experiments provide evidence that the morpho-physiochemical response of rapeseed to bioSeNPs was generally more significant than the relative control and Se (IV) treatments under normal and salt stress conditions. Furthermore, our investigation highlights the considerable efficacy of bioSeNPs to improve seed germination and seedling growth, elevate photosynthesis capacity, secondary metabolism and defense system ability. Our work suggests that retaining the leaf Na^+/K^+ ratio is a component of the mechanisms behind bioSeNPs enabled better plant salt tolerance. Additionally, our results supported that selenation is a more functional method of Se detoxification and vacuole storage is vital for coping with higher Se doses in rapeseed seedlings. The oxidation and transamination of SeCys in rapeseed roots and the conversion of SeCys into SeMet in rapeseed shoots are essential processes for Se detoxification, and selenoproteins degradation is an important way to increase Se tolerance in rapeseed seedling. Taking knowledge gaps into account, these comprehensive comparative data can be helpful to gain novel insights into the benefits or the risk associated with bioSeNPs or Se (IV) function in agriculture and the different pathways of Se detoxification. Additionally, our findings suggested that bioSeNPs is a valuable alternative method for the remediation of reduced growth under abiotic stresses with a novel and eco-friendly technique besides low-cost investment as an advantage, which is a promising material in ameliorating the rapeseed growth and development.

Supplementary Information

The online version contains supplementary material available at <https://doi.org/10.1186/s12951-022-01370-4>.

Additional file 1: Fig. S1. Selenium pathway in plants. **Fig. S2.** Preparation and purification of nano selenium (SeNPs). **Fig. S3.** Effect of different concentrations of SeNPs and Na_2SeO_3 (0, 50, 100 and 150 $\mu\text{mol/L}$) on (a) shoot dry weight (g) and (b) root dry weight (g) on rapeseed seedlings. Bars represent \pm SE of three replicates. The difference in letters indicate significant differences at $P < 0.05$ using Duncan's multiple range tests. **Fig. S4.** (a): Heat map, and A Pearson's correlation of (b): SeNPs and (c) Se (IV) showing the effects of different doses of SeNPs and Se (IV) (0, 50, 100 and 150 $\mu\text{mol/L}$) on the morpho-physiochemical attributes in rapeseed seedlings. Color scale corresponds to the logarithmic transformation of measured values (higher levels are shown in blue, lower levels in red and intermediate levels in dark colors for both blue/red). FG%: final germination percentage; GR: germination rate; VI (I): vigor index I; VI (II): vigor index II; ShL: shoot length; RL: root length; ShFW: shoot fresh weight; RFW: root fresh weight; ShDW: shoot dry weight; RDW: root dry weight; Chl a: chlorophyll a; Chl b: chlorophyll b; TC: total chlorophyll; C: carotenoids content; TSS: total soluble sugar; TP: total protein; MDA: Lipid peroxidation; P: proline content; SOD: super oxidase dismutase; POD: peroxidase; CAT: catalase; APX: ascorbate peroxidase and GR: glutathione reductase. **Fig.**

SS. Impacts of selenium treatments on (a) shoot dry weight (g), and (b) root dry weight (g) on Yangyou 9 under two concentrations of salt stress during the early seedling stage. Bars represent \pm SE of three replicates. The different letters indicate significant differences at $P < 0.05$ using Duncan's multiple range tests. **Table S1.** Sequences of primers used in this study.

Acknowledgements

The authors would like to thank lab members and Abel Wend soo Zongo for their continued support and Ms. G. El-Rewainy for editing the manuscript language and continued support.

Authors' contributions

AME-B and BW: planned and designed the research. AME-B, MB and AH: performed the physiology experiments. AME-B and E-SN: performed the qRT-PCR experiments. AME-B: performed the data curation, formal analysis and software. ASH and HMH: electronic microscopic imaging and analysis AME-B and MB: contributed to writing original draft. AME-B, AH, IM and MA: contributed to review and editing. SZ: provided the experimental material (*Comamonas testosteroni* S44). GZ and BW: responsible for supervision and funding acquisition. All authors read and approved the final manuscript.

Funding

This work was supported by "The National Key Research and Development Program of China, 2018YFD1000900" and "Technical Innovation Project in Hubei Province, 2020BBB061 and 2020BBB062".

Availability of data and materials

Data is contained within the article.

Declarations

Ethics approval and consent to participate

Not applicable.

Consent for publication

All authors consent to publish.

Competing interests

The authors declare that they have no competing financial interests.

Author details

¹MOA Key Laboratory of Crop Ecophysiology and Farming System in the Middle Reaches of the Yangtze River, College of Plant Science & Technology, Huazhong Agricultural University, Wuhan 430070, People's Republic of China. ²Field Crops Research Institute, Agricultural Research Center (ARC), Giza 12619, Egypt. ³Biotechnology Department, Faculty of Agriculture, Al-Azhar University, Cairo 11651, Egypt. ⁴Desert Research Center, Genetics Resource Department, Egyptian Deserts Gene Bank, Cairo 11735, Egypt. ⁵Plant Research Department, Nuclear Research Center, Atomic Energy Authority, Abo Zaabal, Cairo 13795, Egypt. ⁶State Key Laboratory of Agricultural Microbiology, College of Life Science and Technology, Huazhong Agricultural University, Wuhan 430070, People's Republic of China.

Received: 16 December 2021 Accepted: 11 March 2022

Published online: 27 March 2022

References

- Wu C, Dun Y, Zhang Z, Li M, Wu G. Foliar application of selenium and zinc to alleviate wheat (*Triticum aestivum* L.) cadmium toxicity and uptake from cadmium-contaminated soil. *Ecotoxicol Environ Safety*. 2020;190:110091–9.
- Gupta M, Gupta S. An overview of selenium uptake, metabolism, and toxicity in plants. *Front Plant Sci*. 2017;7:1–14.
- Wang X, Cai J, Jiang D, Liu F, Dai T, Cao W. Pre-anthesis high-temperature acclimation alleviates damage to the flag leaf caused by post-anthesis heat stress in wheat. *J Plant Physiol*. 2011;168:585–93.
- Sali A, Zeka D, Fetahu S, Rusinovci I, Kaul H-P. Selenium supply affects chlorophyll concentration and biomass production of maize (*Zea mays* L.). *J Land Manag Food Environ*. 2018;69:249–55.
- Li Y, Zhu N, Liang X, Zheng L, Zhang C, Li Y-F, Zhang Z, Gao Y, Zhao J. A comparative study on the accumulation, translocation and transformation of selenite, selenate, and SeNPs in a hydroponic-plant system. *Ecotoxicol Environ Saf*. 2020;189:109955–61.
- Pilon-Smits EAH, Quinn CF. Selenium metabolism in plants. In: Hell R, Mendel R-R, editors. *Cell biology of metals and nutrients*. Berlin: Springer; 2010. p. 225–41.
- Sors TG, Ellis DR, Na GN, Lahner B, Lee S, Leustek T, Pickering IJ, Salt DE. Analysis of sulfur and selenium assimilation in *Astragalus* plants with varying capacities to accumulate selenium. *Plant J*. 2005;42:785–97.
- Abdel Latef AAH, Abu Alhmad MF, Abdelfattah KE. The possible roles of priming with ZnO nanoparticles in mitigation of salinity stress in lupine (*Lupinus termis*) plants. *J Plant Growth Regul*. 2017;36:60–70.
- Panyuta O, Belava V, Fomaïdi S, Kalinichenko O, Volkogon M, Taran N. The effect of pre-sowing seed treatment with metal nanoparticles on the formation of the defensive reaction of wheat seedlings infected with the eyespot causal agent. *Nanoscale Res Lett*. 2016;11:92–6.
- Ruffini Castiglione M, Giorgetti L, Geri C, Cremonini R. The effects of nano-TiO₂ on seed germination, development and mitosis of root tip cells of *Vicia narbonensis* L. and *Zea mays* L. *J Nanoparticle Res*. 2011;13:2443–9.
- Taran N, Storozhenko V, Svietlova N, Batsmanova L, Shvartau V, Kovalenko M. Effect of zinc and copper nanoparticles on drought resistance of wheat seedlings. *Nanoscale Res Lett*. 2017;12:60–5.
- Mahakham W, Sarmah AK, Maensiri S, Theerakulpisut P. Nanopriming technology for enhancing germination and starch metabolism of aged rice seeds using phytosynthesized silver nanoparticles. *Sci Rep*. 2017;7:8263–9284.
- González-García Y, Cárdenas-Álvarez C, Cadenas-Pliego G, Benavides-Mendoza A, Cabrera-de-la-Fuente M, Sandoval-Rangel A, Valdés-Reyna J, Juárez-Maldonado A. Effect of three nanoparticles (Se, Si and Cu) on the bioactive compounds of bell pepper fruits under saline stress. *Plants*. 2021;10:217–32.
- Hossain Z, Yasmeen F, Komatsu S. Nanoparticles: synthesis, morphophysiological effects, and proteomic responses of crop plants. *Int J Mol Sci*. 2020;21:3056–73.
- Moraru C, Huang Q, Takhistov P, Dogan H, Kokini J. Chapter 21—food nanotechnology: current developments and future prospects. In: Barbosa-Cánovas G, Mortimer A, Lineback D, Spiess W, Buckle K, Colonna P, editors. *Global issues in food science and technology*. San Diego: Academic Press; 2009. p. 369–99.
- Hernandez-Hernandez H, Quiterio-Gutierrez T, Cadenas-Pliego G, Ortega-Ortiz H, Hernandez-Fuentes AD, de la Fuente MC, Valdés-Reyna J, Juárez-Maldonado A. Impact of selenium and copper nanoparticles on yield, antioxidant system, and fruit quality of tomato plants. *Plants*. 2019;8:355–72.
- Khan I, Saeed K, Khan I. Nanoparticles: properties, applications and toxicities. *Arab J Chem*. 2019;12:908–31.
- Zhai X, Zhang C, Zhao G, Stoll S, Ren F, Leng X. Antioxidant capacities of the selenium nanoparticles stabilized by chitosan. *J Nanobiotechnol*. 2017;15:1–12.
- Estevez H, García-Lidon JC, Luque-García JL, Camara C. Effects of chitosan-stabilized selenium nanoparticles on cell proliferation, apoptosis and cell cycle pattern in HepG2 cells: comparison with other selenospecies. *Colloids Surf B*. 2014;122:184–93.
- Hussein H-AA, Darwesh OM, Mekki BB. Environmentally friendly nano-selenium to improve antioxidant system and growth of groundnut cultivars under sandy soil conditions. *Biocatal Agric Biotechnol*. 2019;18:101080–6.
- Hussein H-AA, Darwesh OM, Mekki BB, El-Hallouty SM. Evaluation of cytotoxicity, biochemical profile and yield components of groundnut plants treated with nano-selenium. *Biotechnol Rep*. 2019;24:e00377–83.
- Farouk E-BK, Mahmoud K, El-Senousy WM, Darwesh OM, ElGohary AE. Antiviral/Antimicrobial and schistosomicidal activities of Eucalyptus camaldulensis essential oils. *Int J Pharm Sci Rev Res* 2015, **31**:262–268
- Zsiros O, Nagy V, Párducz Á, Nagy G, Ünneper R, El-Ramady H, Prokisch J, Lisztes-Szabó Z, Fári M, Csajbók J, et al. Effects of selenate and red

- Se-nanoparticles on the photosynthetic apparatus of *Nicotiana tabacum*. *Photosynth Res.* 2019;139:449–60.
24. Hu T, Li H, Li J, Zhao G, Wu W, Liu L, Wang Q, Guo Y. Absorption and bio-transformation of selenium nanoparticles by wheat seedlings (*Triticum aestivum* L.). *Front Plant Sci.* 2018;9:1–10.
 25. Shabala S, Munns R. Salinity stress: physiological constraints and adaptive mechanisms. In: Shabala S, editor. *Plant stress physiology*. Wallingford: CAB; 2017. p. 24–63.
 26. Wangsawang T, Chuamnakhong S, Kohnishi E, Sripichitt P, Sreewongchai T, Ueda A. A salinity-tolerant japonica cultivar has Na⁺ exclusion mechanism at leaf sheaths through the function of a Na⁺ transporter *OsHKT1;4* under salinity stress. *J Agron Crop Sci.* 2018;204:274–84.
 27. Mohamed IAA, Shalby N, El-Badri AMA, Saleem MH, Khan MN, Nawaz MA, Qin M, Agami RA, Kuai J, Wang B, Zhou G. Stomata and xylem vessels traits improved by melatonin application contribute to enhancing salt tolerance and fatty acid composition of *Brassica napus* L. plants. *Agronomy.* 2020;10:1186–208.
 28. Yang Y, Guo Y. Unraveling salt stress signaling in plants. *J Integr Plant Biol.* 2018;60:796–804.
 29. Yang J, Zh Z, Bu Y, Cz R, Jz L, Jj H, Tao C, Zhang K, Xx W, Gx L, et al. Effects of selenium fertilizer on grain yield, Se uptake and distribution in common buckwheat (*Fagopyrum esculentum* Moench). *Plant Soil Environ.* 2015;61:371–7.
 30. Zhu Y, Xie L, Chen GQ, Lee MY, Loque D, Scheller HV. A transgene design for enhancing oil content in *Arabidopsis* and *Camelina* seeds. *Biotechnol Biofuels.* 2018;11:46–56.
 31. Xu D, Yang L, Wang Y, Wang G, Rensing C, Zheng S. Proteins enriched in charged amino acids control the formation and stabilization of selenium nanoparticles in *Comamonas testosteroni* S44. *Sci Rep.* 2018;8:4766–76.
 32. El-Badri AM, Batool M, Wang C, Hashem AM, Tabl KM, Nishawy E, Kuai J, Zhou G, Wang B. Selenium and zinc oxide nanoparticles modulate the molecular and morpho-physiological processes during seed germination of *Brassica napus* under salt stress. *Ecotoxicol Environ Saf.* 2021;225:112695–707.
 33. El-Badri AM, Batool M, Mohamed IAA, Wang Z, Khatib A, Sherif A, Ahmad H, Khan MN, Hassan HM, Elrewayny IM, et al. Antioxidative and metabolic contribution to salinity stress responses in two rapeseed cultivars during the early seedling stage. *Antioxidants.* 2021;10:1227–48.
 34. Chen F, Zhou W, Yin H, Luo X, Chen W, Liu X, Wang X, Meng Y, Feng L, Qin Y, et al. Shading of the mother plant during seed development promotes subsequent seed germination in soybean. *J Exp Bot.* 2020;71:2072–84.
 35. Gill RA, Ali B, Islam F, Farooq MA, Gill MB, Mwamba TM, Zhou W. Physiological and molecular analyses of black and yellow seeded *Brassica napus* regulated by 5-aminolivulinic acid under chromium stress. *Plant Physiol Biochem.* 2015;94:130–43.
 36. Arnon DI. Copper enzymes in isolated chloroplasts. Polyphenoloxidase in *Beta vulgaris*. *Plant Physiol.* 1949;24:1–15.
 37. Hartmut LK, Wellburn AR. Determinations of total carotenoids and chlorophylls a and b of leaf extracts in different solvents. *Biochem Soc Trans.* 1983;11:591–2.
 38. Bradford MM. A rapid and sensitive method for the quantitation of microgram quantities of protein utilizing the principle of protein-dye binding. *Anal Biochem.* 1976;72:248–54.
 39. Wen C, Dong A, Li G, Lei S, Lei Y. Determination of total sugar and reducing sugar in *Viola philippicasp* Munda W. Becker by anthrone colorimetry. *Mod Food Sci Technol.* 2005;21:122–4.
 40. Ahanger MA, Agarwal RM. Potassium up-regulates antioxidant metabolism and alleviates growth inhibition under water and osmotic stress in wheat (*Triticum aestivum* L.). *Protoplasma.* 2017;254:1471–86.
 41. Bates LS, Waldren RP, Teare I. Rapid determination of free proline for water-stress studies. *Plant Soil.* 1973;39:205–7.
 42. Ulhassan Z, Gill RA, Ali S, Mwamba TM, Ali B, Wang J, Huang Q, Aziz R, Zhou W. Dual behavior of selenium: Insights into physio-biochemical, anatomical and molecular analyses of four *Brassica napus* cultivars. *Chemosphere.* 2019;225:329–41.
 43. Hashem AM, Moore S, Chen S, Hu C, Zhao Q, Elesawi IE, Feng Y, Topping JF, Liu J, Lindsey K, Chen C. Putrescine depletion affects arabidopsis root meristem size by modulating auxin and cytokinin signaling and ROS accumulation. *Int J Mol Sci.* 2021;22:4094–111.
 44. Ling H, Zeng X, Guo S. Functional insights into the late embryogenesis abundant (LEA) protein family from *Dendrobium officinale* (Orchidaceae) using an *Escherichia coli* system. *Sci Rep.* 2016;6:39693–701.
 45. Handa N, Kohli SK, Sharma A, Thukral AK, Bhardwaj R, Abd-Allah EF, Alqarawi AA, Ahmad P. Selenium modulates dynamics of antioxidative defence expression, photosynthetic attributes and secondary metabolites to mitigate chromium toxicity in *Brassica juncea* L. plants. *Environ Exp Bot.* 2019;161:180–92.
 46. Xu C, Zhang S, Chuang C-y, Miller EJ, Schwehr KA, Santschi PH. Chemical composition and relative hydrophobicity of microbial exopolymeric substances (EPS) isolated by anion exchange chromatography and their actinide-binding affinities. *Mar Chem.* 2011;126:27–36.
 47. Jain R, Jordan N, Weiss S, Foersterdorf H, Heim K, Kacker R, Hübner R, Kramer H, van Hullebusch ED, Farges F, Lens PNL. Extracellular polymeric substances govern the surface charge of biogenic elemental selenium nanoparticles. *Environ Sci Technol.* 2015;49:1713–20.
 48. Bajaj M, Schmidt S, Winter J. Formation of Se (0) NANOPARTICLES by *Duganella* sp. and *Agrobacterium* sp. isolated from Se-laden soil of North-East Punjab, India. *Microb Cell Factories.* 2012;11:64–77.
 49. Yang T, Fang GY, He H, Chen J. Genome-wide identification, evolutionary analysis and expression profiles of LATERAL ORGAN BOUNDARIES DOMAIN gene family in *Lotus japonicus* and *Medicago truncatula*. *PLoS ONE.* 2016;11:e0161901–15.
 50. Bashandy T, Guillemot J, Vernoux T, Caparros-Ruiz D, Ljung K, Meyer Y, Reichheld JP. Interplay between the NADP-linked thioredoxin and glutathione systems in *Arabidopsis* auxin signaling. *Plant Cell.* 2010;22:376–91.
 51. Hirschmann F, Krause F, Papenbrock J. The multi-protein family of sulfotransferases in plants: composition, occurrence, substrate specificity, and functions. *Front Plant Sci.* 2014;5:556–68.
 52. Liu Y, Zhang L, Chen L, Ma H, Ruan Y, Xu T, Xu C, He Y, Qi M. Molecular cloning and expression of an encoding galactinol synthase gene (*AnGol51*) in seedling of *Ammopiptanthus nanus*. *Sci Rep.* 2016;6:36113–23.
 53. Eklöf JM, Brumer H. The XTH gene family: an update on enzyme structure, function, and phylogeny in xyloglucan remodeling. *Plant Physiol.* 2010;153:456–66.
 54. Juárez-Maldonado A, Ortega-Ortiz H, Morales-Díaz AB, González-Morales S, Morelos-Moreno Á, De la Fuente MC, Sandoval-Rangel A, Cadenas-Pliego G, Benavides-Mendoza A. Nanoparticles and nanomaterials as plant biostimulants. *Int J Mol Sci.* 2019;20:1–19.
 55. Zuverza-Mena N, Martínez-Fernández D, Du W, Hernández-Viezas JA, Bonilla-Bird N, López-Moreno ML, Komárek M, Peralta-Videa JR, Gardea-Torresdey JL. Exposure of engineered nanomaterials to plants: Insights into the physiological and biochemical responses—a review. *Plant Physiol Biochem.* 2017;110:236–64.
 56. Hillegass JM, Shukla A, Lathrop SA, MacPherson MB, Fukagawa NK, Mossman BT. Assessing nanotoxicity in cells in vitro. *WIREs Nanomed Nanobiotechnol.* 2010;2:219–31.
 57. Morales-Espinoza MC, Cadenas-Pliego G, Perez-Alvarez M, Hernandez-Fuentes AD, de la Fuente MC, Benavides-Mendoza A, Valdes-Reyna J, Juarez-Maldonado A. Se nanoparticles induce changes in the growth, antioxidant responses, and fruit quality of tomato developed under NaCl stress. *Molecules.* 2019;24:3030–46.
 58. Khan MR, Adam V, Rizvi TF, Zhang B, Ahamad F, Joško I, Zhu Y, Yang M, Mao C. Nanoparticle-plant interactions: two-way traffic. *Small.* 2019;15:1901794–813.
 59. Sotoodehnia-Korani S, Iranbakhsh A, Ebadi M, Majd A, Ardebili ZO. Selenium nanoparticles induced variations in growth, morphology, anatomy, biochemistry, gene expression, and epigenetic DNA methylation in *Capsicum annum*; an in vitro study. *Environ Pollut.* 2020. <https://doi.org/10.1016/j.envpol.2020.114727>.
 60. Domokos-Szabolcsy E, Marton L, Sztrik A, Babka B, Prokisch J, Fari M. Accumulation of red elemental selenium nanoparticles and their biological effects in *Nicotinia tabacum*. *Plant Growth Regul.* 2012;68:525–31.
 61. Zhang L, Li Q, Yang X, Xia Z. Effects of sodium selenite and germination on the sprouting of chickpeas (*Cicer arietinum* L.) and its content of selenium, formononetin and biochanin A in the sprouts. *Biol Trace Elem Res.* 2012;146:376–80.

62. Molnár Á, Kolbert Z, Kéri K, Feigl G, Ördög A, Szöllösi R, Erdei L. Selenite-induced nitro-oxidative stress processes in *Arabidopsis thaliana* and *Brassica juncea*. *Ecotoxicol Environ Saf*. 2018;148:664–74.
63. Wang M, Peng Q, Zhou F, Yang W, Dinh QT, Liang D. Uptake kinetics and interaction of selenium species in tomato (*Solanum lycopersicum* L.) seedlings. *Environ Sci Pollut Res*. 2019;26:9730–8.
64. Van Hoewyk D. A tale of two toxicities: malformed selenoproteins and oxidative stress both contribute to selenium stress in plants. *Ann Bot*. 2013;112:965–72.
65. Falco WF, Queiroz AM, Fernandes J, Botero ER, Falcão EA, Guimarães FEG, M'Peko JC, Oliveira SL, Colbeck I, Caires ARL. Interaction between chlorophyll and silver nanoparticles: a close analysis of chlorophyll fluorescence quenching. *J Photochem Photobiol A*. 2015;299:203–9.
66. Queiroz AM, Mezacasava AV, Graciano DE, Falco WF, M'Peko JC, Guimarães FEG, Lawson T, Colbeck I, Oliveira SL, Caires ARL. Quenching of chlorophyll fluorescence induced by silver nanoparticles. *Spectrochim Acta Part A Mol Biomol Spectrosc*. 2016;168:73–7.
67. Santos ESD, Graciano DE, Falco WF, Caires ARL, Arruda EJDE. Effects of copper oxide nanoparticles on germination of *Sesbania virgata* (FABACEAE) plants. *An Acad Bras Cienc*. 2021;93:e20190739–52.
68. Salama HMH. Effects of silver nanoparticles in some crop plants, Common bean (*Phaseolus vulgaris* L.) and corn (*Zea mays* L.). *Int Res J Biotechnol*. 2012;3:190–7.
69. Mohsenzadeh S, Moosavian SS. Zinc sulphate and nano-zinc oxide effects on some physiological parameters of *Rosmarinus officinalis*. *Am J Plant Sci*. 2017;8:2635–49.
70. Mostofa MG, Hossain MA, Siddiqui MN, Fujita M, Tran LS. Phenotypical, physiological and biochemical analyses provide insight into selenium-induced phytotoxicity in rice plants. *Chemosphere*. 2017;178:212–23.
71. Abbas SM. Effects of low temperature and selenium application on growth and the physiological changes in sorghum seedlings. *J Stress Physiol Biochem*. 2012;8:268–86.
72. Parvaiz A, Allah EFA, Abeer H, Maryam S, Salih G. Exogenous application of selenium mitigates cadmium toxicity in *Brassica juncea* L. (czern & cross) by up-regulating antioxidative system and secondary metabolites. *J Plant Growth Regul*. 2012;8:268–86.
73. Ze Y, Liu C, Wang L, Hong M, Hong F. The regulation of TiO₂ nanoparticles on the expression of light-harvesting complex II and photosynthesis of chloroplasts of *Arabidopsis thaliana*. *Biol Trace Elem Res*. 2011;143:1131–41.
74. Smirnoff N. Chapter 4—vitamin C: the metabolism and functions of ascorbic acid in plants. In: Rébeillé F, Douce R, editors. *Advances in botanical research*, vol. 59. Cambridge: Academic Press; 2011. p. 107–77.
75. Zahedi SM, Abdelrahman M, Hosseini MS, Hoveizeh NF, Tran L-SP. Alleviation of the effect of salinity on growth and yield of strawberry by foliar spray of selenium-nanoparticles. *Environ Pollut*. 2019;253:246–58.
76. Abdel Latef AA, Tran L-SP. Impacts of priming with silicon on the growth and tolerance of maize plants to alkaline stress. *Front Plant Sci*. 2016;7:1–10.
77. Jain R, Verma R, Singh A, Chandra A, Solomon S. Influence of selenium on metallothionein gene expression and physiological characteristics of sugarcane plants. *Plant Growth Regul*. 2015;77:109–15.
78. Babajani A, Iranbakhsh A, Oraghi Ardebili Z, Eslami B. Differential growth, nutrition, physiology, and gene expression in *Melissa officinalis* mediated by zinc oxide and elemental selenium nanoparticles. *Environ Sci Pollut Res*. 2019;26:24430–44.
79. Hawrylak-Nowak B. Comparative effects of selenite and selenate on growth and selenium accumulation in lettuce plants under hydroponic conditions. *Plant Growth Regul*. 2013;70:149–57.
80. Choudhury FK, Rivero RM, Blumwald E, Mittler R. Reactive oxygen species, abiotic stress and stress combination. *Plant J*. 2017;90:856–67.
81. Nazerieh H, Oraghi Ardebili Z, Iranbakhsh A. Potential benefits and toxicity of nanoselenium and nitric oxide in peppermint. *Acta Agric Slov*. 2018;111:357–68.
82. Safari M, Oraghi Ardebili Z, Iranbakhsh A. Selenium nano-particle induced alterations in expression patterns of heat shock factor A4A (HSFA4A), and high molecular weight glutenin subunit 1Bx (Glu-1Bx) and enhanced nitrate reductase activity in wheat (*Triticum aestivum* L.). *Acta Physiol Plant*. 2018;40:117–24.
83. Quiterio-Gutierrez T, Ortega-Ortiz H, Cadenas-Pliego G, Hernandez-Fuentes AD, Sandoval-Rangel A, Benavides-Mendoza A, de la Fuente MC, Juarez-Maldonado A. The application of selenium and copper nanoparticles modifies the biochemical responses of tomato plants under stress by *Alternaria solani*. *Int J Mol Sci*. 2019;20:1950–65.
84. Raigond P, Baswaraj R, Bhawana K, Brajesh S, Alka J, Som D. Effect of zinc nanoparticles on antioxidative system of potato plants. *J Environ Biol*. 2017;38:435–9.
85. Li ZG. Methylglyoxal and glyoxalase system in plants: old players new concepts. *Bot Rev*. 2016;82:183–203.
86. Ahanger MA, Tomar NS, Tittal M, Aargal S, Agarwal RM. Plant growth under water/salt stress: ROS production; antioxidants and significance of added potassium under such conditions. *Physiol Mol Biol Plants*. 2017;23:731–44.
87. Ghazi D. The contribution of nano-selenium in alleviation of salinity adverse effects on coriander plants. *J Soil Sci Agric Eng*. 2018;9:753–60.
88. Rossi L, Zhang W, Ma X. Cerium oxide nanoparticles alter the salt stress tolerance of *Brassica napus* L. by modifying the formation of root apoplastic barriers. *Environ Pollut*. 2017;229:132–8.
89. Zhang Y, Wang L, Liu Y, Zhang Q, Wei Q, Zhang W. Nitric oxide enhances salt tolerance in maize seedlings through increasing activities of proton-pump and Na⁺/H⁺ antiport in the tonoplast. *Planta*. 2006;224:545–55.
90. Habibi G. Selenium ameliorates salinity stress in *Petroselinum crispum* by modulation of photosynthesis and by reducing shoot Na accumulation. *Russ J Plant Physiol*. 2017;64:368–74.
91. Wu H, Zhang X, Giraldo JP, Shabala S. It is not all about sodium: revealing tissue specificity and signalling roles of potassium in plant responses to salt stress. *Plant Soil*. 2018;431:1–17.
92. Liu J, Li G, Chen L, Gu J, Wu H, Li Z. Cerium oxide nanoparticles improve cotton salt tolerance by enabling better ability to maintain cytosolic K⁺/Na⁺ ratio. *J Nanobiotechnol*. 2021;19:153–68.
93. Handa N, Bhardwaj R, Kaur H, Poonam, Kapoor D, Rattan A, Kaur S, Thukral AK, Kaur S, Arora S, Kapoor N. Chapter 7—selenium: An antioxidant protectant in plants under stress. In: Ahmad P, editor. *Plant metal interaction*. Amsterdam: Elsevier; 2016. p. 179–207.
94. Valdez Barillas JR, Quinn CF, Freeman JL, Lindblom SD, Marcus MA, Gilligan TM, Alford ER, Wangeline AL, Pilon-Smits EAH. Selenium distribution and speciation in the hyperaccumulator *Astragalus bisulcatus* and associated ecological partners. *Plant Physiol*. 2012;159:1834–44.
95. Gong Z, Xiong L, Shi H, Yang S, Herrera-Estrella LR, Xu G, Chao DY, Li J, Wang PY, Qin F, et al. Plant abiotic stress response and nutrient use efficiency. *Sci China Life Sci*. 2020;63:635–74.
96. Burla B, Pfrunder S, Nagy R, Francisco RM, Lee Y, Martinoia E. Vacuolar transport of abscisic acid glucosyl ester is mediated by ATP-binding cassette and proton-antiport mechanisms in arabidopsis. *Plant Physiol*. 2013;163:1446–58.
97. Sabbagh M, Van Hoewyk D. Malformed selenoproteins are removed by the ubiquitin-proteasome pathway in *Stanleya pinnata*. *Plant Cell Physiol*. 2012;53:555–64.
98. Okumoto S, Koch W, Tegeder M, Fischer WN, Biehl A, Leister D, Stierhof YD, Frommer WB. Root phloem-specific expression of the plasma membrane amino acid proton co-transporter AAP3. *J Exp Bot*. 2004;55:2155–68.
99. Vallentine P, Hung C-Y, Xie J, Van Hoewyk D. The ubiquitin-proteasome pathway protects *Chlamydomonas reinhardtii* against selenite toxicity, but is impaired as reactive oxygen species accumulate. *AoB PLANTS*. 2014;6:1–11.
100. Zhou Y, Qiaoyu T, Meiru W, Di M, Hui L, Shouchuang W, Chi Z, Li D, Jie L. Comparative transcriptomics provides novel insights into the mechanisms of selenium tolerance in the hyperaccumulator plant *Cardamine hupingshanensis*. *Sci Rep*. 2018;8:2789–805.

Publisher's Note

Springer Nature remains neutral with regard to jurisdictional claims in published maps and institutional affiliations.